ORGANOMETALLICS

pubs.acs.org/Organometallics

Article

Rhodium and Iridium Complexes of Lutidine-Based NHC/Amino Pincer Ligands: From Monodentate to Tetradentate Coordination Enabled by C−H Activation

Miguel González-Lainez, M. Victoria Jiménez,* Vincenzo Passarelli, F. Javier Modrego, and Jesús J. Pérez-Torrente*

Cite This: *Organometallics* 2023, 42, 3292−3306

Read Online

ABSTRACT: A series of rhodium and iridium complexes derived from lutidine-based ligands (lutidine, 2,6-dimethylpyridine) with NHC and amino side-donor functions have been prepared and characterized. Deprotonation of the functionalized imidazolium salts, [^{t}BuHImCH$_2$PyCH$_2$NR$_2$]Br, by the bridging methoxo ligands of the dinuclear complexes [M(μ-OMe)(cod)]$_2$ affords [MBr(cod)(κC-^{t}BuImCH$_2$PyCH$_2$NR$_2$)] (M = Rh and Ir) complexes from which a series of Rh(I) and Ir(I) complexes including [M(cod)($\kappa^3 C,N,N'$-^{t}BuImCH$_2$PyCH$_2$NR$_2$)]$^+$, [Rh(CO)($\kappa^3 C,N,N'$-^{t}BuImCH$_2$PyCH$_2$NR$_2$)]$^+$, and [IrBr(CO)$_2$(κC-^{t}BuImCH$_2$PyCH$_2$NR$_2$)] are readily accessible by halide abstraction and/or carbonylation reactions. In contrast, direct metalation of imidazolium salts with the dinuclear compounds [M(μ-Cl)(cod)]$_2$ (M = Rh and Ir) in the presence of potassium acetate and potassium iodide, a well-established synthetic route to M(III) species, provides access to unusual di-iodido M(III) cyclometalated compounds [MI$_2$\{$\kappa^4 C,C',N,N'$-(CH$_2$CMe$_2$ImCH$_2$PyCH$_2$NR$_2$)\}] in low yield. Experimental studies combined with DFT calculations suggest that cyclometalated M(III) hydrido [MH(CH$_3$CN)\{$\kappa^4 C,C',N,N'$-(CH$_2$CMe$_2$ImCH$_2$PyCH$_2$NR$_2$)\}]$^+$ compounds and square-planar cyclometalated M(I) [M\{$\kappa^4 C,C',N,N'$-(CH$_2$CMe$_2$ImCH$_2$PyCH$_2$NR$_2$)\}] species resulting from their deprotonation by acetate could be intermediates involved in the formation of these compounds. Based on the observed formation of elemental rhodium, disproportionation of square-planar cyclometalated M(I) complexes to afford M(0) and the cationic M(II) species [M\{$\kappa^4 C,C',N,N'$-(CH$_2$CMe$_2$ImCH$_2$PyCH$_2$NR$_2$)\}]$^+$ is proposed. Reaction of the latter with iodide (I$^-$) would regenerate the M(I) intermediate to give an iodo radical (I•) that in turn could dimerize to form diiodine I$_2$. In this regard, DFT calculations have shown that the oxidative addition of diiodine to the cyclometalated M(I) intermediates leading to the di-iodido M(III) cyclometalated compounds is a highly exergonic process.

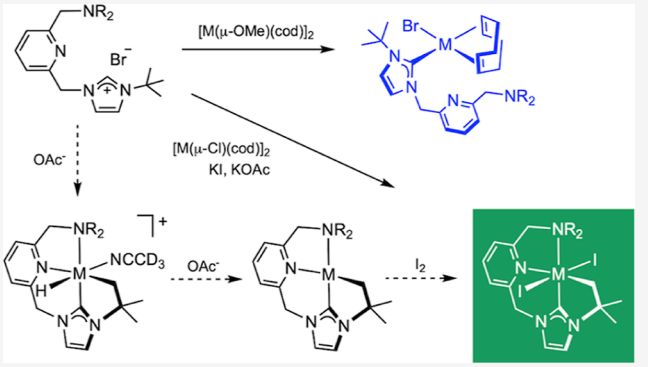

INTRODUCTION

Pincer-type ligands have become increasingly important in transition metal chemistry. Their unique structural and electronic properties make them highly versatile and valuable tools for a broad range of applications such as supramolecular chemistry, materials science, and catalysis.[1,2] On the other hand, *N*-heterocyclic carbenes (NHCs) have emerged as powerful ligands in modern chemistry owing to their strong coordination ability, topological versatility, and tunable electronic and steric properties.[3] The incorporation of NHCs into well-established pincer ligand platforms has attracted considerable interest in recent years. The stability provided by the pincer framework in combination with the strong σ-donor character of the NHC moiety results in more robust metal complexes suitable for a wide range of catalytic transformations.[4] In addition, the ease of functionalization of the NHC fragment also allows the properties of the metal center to be fine-tuned.

Metal complexes based on lutidine-derived pincer ligands are amenable to structural modification by reversible deprotonation of the methylene arms of the ligand, accompanied by dearomatization of the pyridine ring. This structural pattern allows the activation of a variety of X−H (X = H, C, O, and N) bonds by metal−ligand cooperation, which has important implications for catalysis.[5] In this context,

Received: September 18, 2023
Revised: October 12, 2023
Accepted: October 18, 2023
Published: November 2, 2023

lutidine-derived CNC pincer complexes having two NHCs as flanking donors are currently the focus of extensive research.[6] Late transition metal CNC pincer complexes have been shown to be efficient catalysts in a number of transformations, including hydrogenation/dehydrogenation and cross-coupling reactions, some of which involve metal−ligand cooperation.[7] Nonsymmetric lutidine-derived CNZ pincer complexes combining an NHC moiety with a different donor function (Z = N, P, and O) have been recently reported (Figure 1). Rhodium, iridium, ruthenium, palladium, and copper pincer complexes derived from this type of ligand have been used in many catalytic applications.[8]

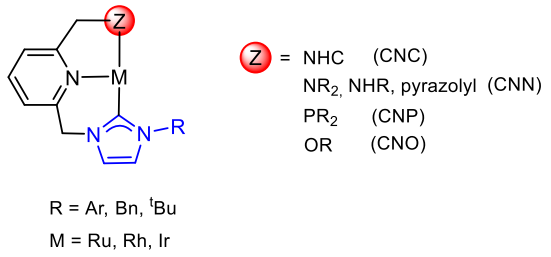

Figure 1. Structure of lutidine-derived CNZ pincer complexes.

Iglesias, Sánchez et al. first reported in 2010 the synthesis of rhodium, palladium, and gold CNN pincer complexes featuring an *S*-proline functional group (proline, pyrrolidine-2-carboxylic acid) and their application in asymmetric hydrogenation.[9] Soon thereafter, the same group reported the synthesis of chiral rhodium and ruthenium CNN pincer complexes having pyrrolidine-2-carboxamide or dialkylamino groups functionalized with a pendant alkoxysilane. The silyl group was used to immobilize the complexes by covalent bonding to mesoporous silica MCM-41 to prepare efficient and recoverable catalysts with applications in asymmetric hydrogenation and hydrogen transfer reactions.[10] Molecular Ru−CNN pincer complexes having a diethylamino functional group were found to be efficient catalysts for ester hydrogenation under mild conditions.[11] Copper-based coordination polymers based on a related diethylamino-functionalized ligand showed remarkable activity in azide−alkyne cycloaddition reactions under base-free conditions (CuAAC).[12] Pincer iridium and ruthenium complexes featuring a secondary amino −NHR functional group behave as dual proton-responsive ligands and have found application in ammonia-borane dehydrogenation and (de)hydrogenation of *N*-heterocycle reactions, respectively.[13] On the other hand, pyrazolyl-functionalized Pd−CNN pincer complexes were found to be efficient catalysts in Suzuki−Miyaura reactions.[14] Palladium and iridium CNP pincer complexes having a phosphine functional group were first reported by Paneque, Suárez et al. in 2016.[15] These electron−rich complexes exhibited a distinct reactivity, including dimerization, C−H bond activation, and hydrogenation of the NHC skeleton.[16] Catalytic applications of these Ir−CNP pincer complexes include the hydroboration of carbon dioxide and the hydrogenation of aldehydes.[17] Our research group has recently disclosed the hemilabile behavior of pincer ligands with a methoxy functional group. The iridium CNO complexes showed excellent catalytic activity in the *N*-methylation of nitroarenes and amines using methanol as a reducing agent and C1 source, while related rhodium complexes proved to be *β*-(*Z*)-selective alkyne hydrosilylation catalysts.[18]

The results described above show that the development of nonsymmetric lutidine-derived CNX pincer metal complexes has been driven by their applications in catalysis and reactivity studies of species resulting from dearomatization processes. However, the detailed study of the coordination chemistry of such ligands has been largely overlooked. We report herein on the synthesis of rhodium(I) and iridium(I) complexes of lutidine-derived NHC/amino functionalized ligands, in which the ligand exhibits different coordination modes depending on the auxiliary ligands on the metal center. In addition, the direct metalation of the imidazolium salt precursors using a well-established procedure for bis-NHC complexes has led to the preparation of unprecedented Rh(III) and Ir(III) di-iodido complexes in which the pincer ligand exhibits a tetradentate coordination as a result of C−H activation at the NHC wingtip.

RESULTS AND DISCUSSION

Synthesis of Rhodium and Iridium Complexes Bearing *N,N*-Functionalized NHC Ligands. The direct deprotonation of the imidazolium salt [^{t}BuHImCH$_2$PyCH$_2$NEt$_2$]Br by the bridging methoxo ligands of the dinuclear complexes [M(*μ*-OMe)(cod)]$_2$ (M = Rh and Ir) afforded yellow solutions from which the neutral bromo-complexes [RhBr(cod)(*κC*-^{t}BuImCH$_2$PyCH$_2$NEt$_2$)] (**1**) and [IrBr(cod)-(*κC*-^{t}BuImCH$_2$PyCH$_2$NEt$_2$)] (**2**) were isolated as yellow solids in good yields (Scheme 1a). The synthesis of [RhBr(cod)(*κC*-^{t}BuImCH$_2$PyCH$_2$NH^{t}Bu)] (**3**) from the

Scheme 1. Synthesis of Complexes [MBr(cod)(*κC*-^{t}BuImCH$_2$PyCH$_2$NEt$_2$)] and [M(cod)(*κ*^{3}*C,N,N′*-^{t}BuImCH$_2$PyCH$_2$NEt$_2$)]$^+$

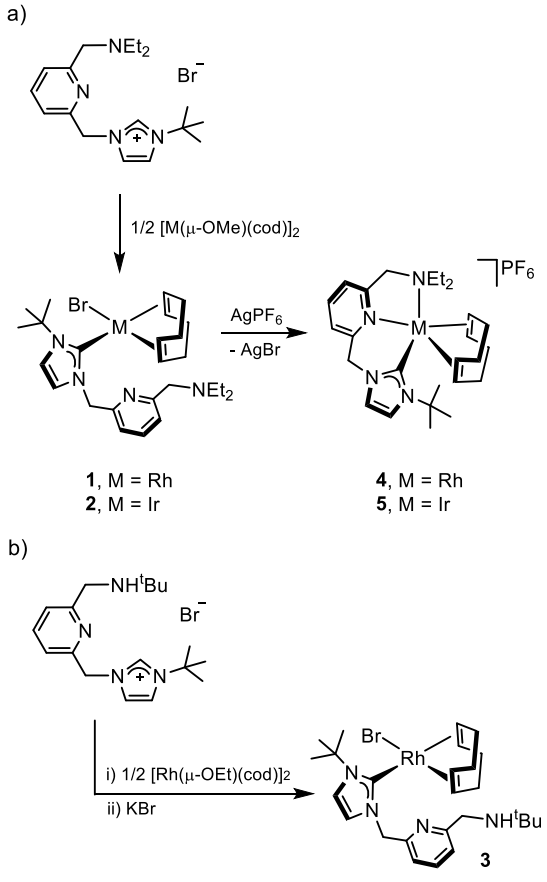

https://doi.org/10.1021/acs.organomet.3c00403
Organometallics 2023, 42, 3292−3306

related imidazolium salt [^{t}BuHImCH$_2$PyCH$_2$NH^{t}Bu]Br proved to be problematic by this method, so we followed the synthetic strategy described by Herrmann et al. using the dinuclear compound [Rh(μ-OEt)(cod)]$_2$ prepared in situ by the reaction of [Rh(μ-Cl)(cod)]$_2$ with an excess of NaH in ethanol (Scheme 1b).[19] However, ^{1}H NMR analysis of the isolated yellow solid revealed the presence of a mixture of the neutral bromo- and chloro-complexes, in which the former predominates (70%). Metathesis reaction with an excess of KBr in dichloromethane and efficient removal of the inorganic salts cleanly afforded **3** as a yellow solid in 60% yield.

The spectroscopic data for these complexes are consistent with a square planar structure resulting from the coordination of a bromido ligand and the NHC moiety of the polydentate ligand with uncoordinated pyridine and amino fragments. The formation of the M−NHC bond was confirmed by the absence of the characteristic low-field ^{1}H signal assigned to the NCHN (H2) proton of the imidazolium salt precursors and the presence of a ^{13}C doublet for **1** and **3** ($J_{Rh-C} \approx 50$ Hz) and a singlet for **2** at around δ 180 ppm, which were assigned to the carbenic carbon atom. The diasterotopic protons of the Im-CH$_2$−Py methylene linker were observed as two well-separated doublets in the ^{1}H NMR spectra with $J_{H-H} \approx 15$ Hz. In addition, the =CH groups of the cod ligand showed four distinct resonances in both the ^{1}H and ^{13}C{^{1}H} NMR spectra, suggesting restricted rotation around the M−C$_{NHC}$ bond. The =CH trans to the NHC moiety were observed to be more unshielded in both spectra, with smaller J_{Rh-C} coupling constants, compared to the =CH protons trans to bromo.[20] However, the protons of the Py-CH$_2$−NR$_2$ methylene linker were isochronous and appeared as a singlet around δ 3.7 ppm, probably due to the conformational freedom of the amino fragment away from the metal center.

Reaction of the neutral bromo-complexes **1** and **2** with an equivalent of AgPF$_6$ in dichloromethane resulted in the precipitation of AgBr and formation of yellow solutions of the cationic complexes [Rh(cod)(κ^3*C,N,N*′-^{t}BuImCH$_2$-PyCH$_2$NEt$_2$)]PF$_6$ (**4**) and [Ir(cod)-(κ^3*C,N,N*′-^{t}BuImCH$_2$PyCH$_2$NEt$_2$)]PF$_6$ (**5**), which were isolated as yellow and pale brown microcrystalline solids, respectively, in 70−75% yield (Scheme 1). Conductivity measurements of nitromethane solutions confirmed that both compounds are 1:1 electrolytes.

The abstraction of the bromido ligand creates a coordination vacancy that should be occupied by the pyridine fragment of the functionalized NHC ligand, thus adopting a κ^2*C,N* coordination mode. However, the molecular structure of **5** determined by an X-ray diffraction study evidenced a κ^3*C,N,N*′ coordination derived from the coordination of the amino fragment to the metal center (Figure 2). Indeed, the crystal structure of **5** shows a pentacoordinate metal center with a severely distorted trigonal bypiramidal geometry. The cod ligand spans one axial and one equatorial position [CT02-Ir1-CT01 85.685(4)°], and a highly strained facial κ^3*C,N,N*′ coordination is observed for the lutidine-derived ligand with the NHC moiety in the remaining axial position [C1−Ir1 2.064(3), N12−Ir1 2.213(2), and N18−Ir1 2.545(2) Å]. Reasonably, the small bite angle N12−Ir−N18 [69.07(8)°] brings about elongated Ir1−N12 [2.213(2) Å] and Ir1−N18 [2.545(2) Å] bond lengths. Similarly, as a consequence of the reduced bite angle N12−Ir1−C1 [82.32(9)°], the NHC moiety significantly deviates from the ideal arrangement with respect to the Ir1−C1 bond (pitch, θ 4.5°; yaw, ψ 13.9°).

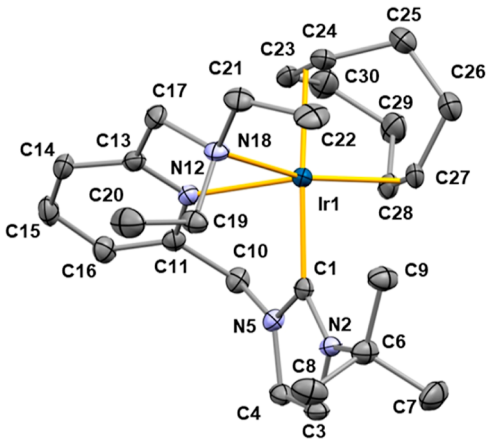

Figure 2. ORTEP view of [Ir(cod)-(κ^3*C,N,N*′-^{t}BuImCH$_2$PyCH$_2$NEt$_2$)]$^+$ in **5**. Thermal ellipsoids are at 50% probability, and hydrogen atoms are omitted for clarity. Selected bond lengths (Å) and angles (deg) are: C1−Ir1 2.064(3), N12−Ir1 2.213(2), N18−Ir1 2.545(2), C23−C24 1.390(4), C27−C28 1.443(4), C1−Ir1−N12 82.32(9), C1−Ir1−N18 101.19(9), N12−Ir1−N18 69.07(8), Ir1-CT02 1.95402(12), Ir1-CT01 2.08747(12), CT02-Ir1-CT01 85.685(4), C1−Ir1−CT01 166.25(7), CT02−Ir1−N12 143.43(6), and CT02−Ir1−N18 147.51(5). CT01 and CT02 are the centroids of C23 and C24, and of C27 and C28, respectively.

The NMR spectra evidence that the coordination of the amino fragments in both complexes is maintained in solution. For comparative purposes, the ^{1}H NMR spectra of compounds **2** and **5** are shown in Figure 3. The protons of the Py-CH$_2$−NEt$_2$ methylene linker, observed as a singlet in **2**, appear as two doublets at δ 4.18 and 3.80 ppm (J_{H-H} = 15.1 Hz) in **5** due to conformational restriction resulting from the coordination of the pyridine fragment.[18b] Moreover, the >CH$_2$ of the ethyl substituents of the -NEt$_2$ fragment, observed as a quartet in the spectrum of **2**, appear as two multiplets in the spectrum of **5**, which is a diagnostic of the coordination of the -NEt group to the iridium center.

Carbonylation of [MBr(cod)(κC-^{t}BuImCH$_2$PyCH$_2$NR$_2$)] (M = Rh and Ir). Bubbling of CO(g) through solutions of neutral rhodium complexes **1** and **3** in toluene gave yellow solutions of compounds [Rh(CO)(κ^3*C,N,N*′-^{t}BuImCH$_2$-PyCH$_2$NEt$_2$)]Br (**6**) and [Rh(CO)-(κ^3*C,N,N*′-^{t}BuImCH$_2$PyCH$_2$NH^{t}Bu)]Br (**7**), which were isolated as yellow microcrystalline solids in 60−70% yield. Substitution of the cod ligand by carbon monoxide induces the coordination of the pyridine and amino fragments of the ligands, yielding cationic rhodium(I) compounds with pincer structure and a single carbonyl ligand (Scheme 2).

The carbonyl ligand was observed as a strong stretching ν(CO) band at 1946 (**6**) and 1947 cm^{-1} (**7**) in the ATR-IR spectra. On the other hand, conductivity measurements of the complexes in nitromethane agree with 1:1 electrolytes, confirming the cationic nature of the complexes. The ^{1}H NMR spectra of both compounds suggest a square planar structure. Thus, the protons of both >CH$_2$ linkers in **6** appeared with singlet multiplicity in agreement with the average C_s symmetry. However, two broad resonances were observed for **7**, which is consistent with its asymmetric structure due to the presence of the NH^{t}Bu fragment. The ^{13}C{^{1}H}-apt NMR spectra of both compounds showed two doublets in the low-field region. The less shielded signal, at δ 193.2 (J_{Rh-C} = 81.2 Hz) in **6** and 195.4 ppm (J_{Rh-C} = 79.8 Hz)

https://doi.org/10.1021/acs.organomet.3c00403
Organometallics 2023, 42, 3292−3306

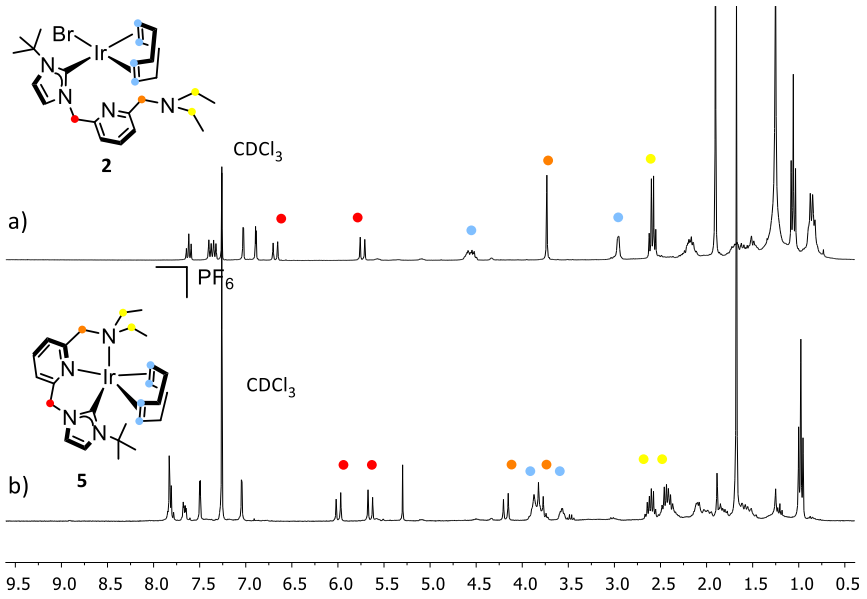

Figure 3. Comparison of the ^{1}H NMR spectra of complexes **2** and **5** ($CDCl_3$).

Scheme 2. Synthesis of Complexes [Rh(CO)(κ^3*C,N,N′*-^{t}BuImCH$_2$PyCH$_2$NRR′)] and [IrBr(CO)$_2$(κ*C*-^{t}BuImCH$_2$PyCH$_2$NEt$_2$)]

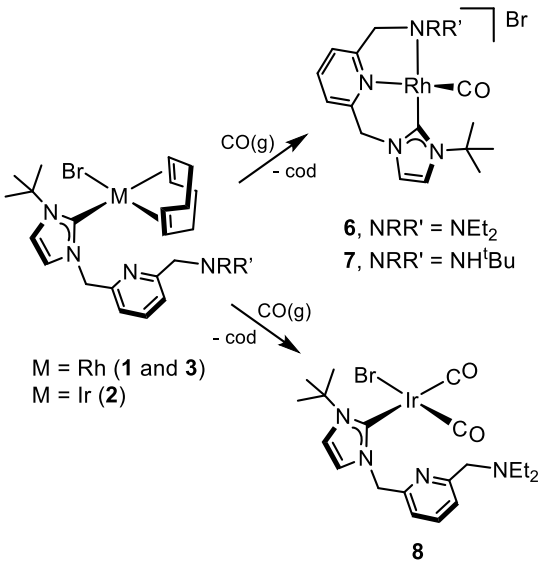

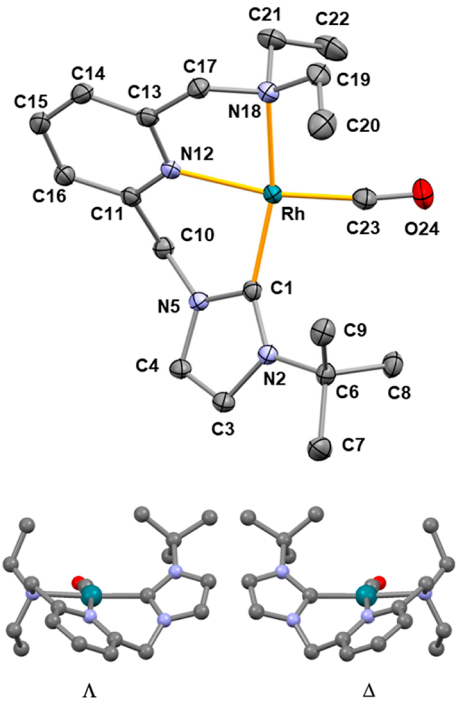

Figure 4. (Top) ORTEP view of [Rh(CO)(κ^3*C,N,N′*^{t}BuImCH$_2$PyCH$_2$NEt$_2$)]$^+$ in **6**. Thermal ellipsoids are at 50% probability, and hydrogen atoms are omitted for clarity. Selected bond lengths (Å) and angles (deg) are: C1−Rh 2.029(2), N12−Rh 2.0875(17), N18−Rh 2.1579(18), C23−Rh 1.816(2), C23−O24 1.154(3), C1−Rh−N12 89.05(8), C23−Rh−N12 167.43(9), C23−Rh−N18 94.73(9), C1−Rh−N18 165.17(8), N12−Rh−N18 78.39(7), C23−Rh−C1 99.02(9), and O24−C23−Rh 172.1(2). (bottom) View of the Δ and Λ enantiomers in **6**.

in **7**, corresponds to the carbonyl ligand, whereas the second one corresponds to the carbene carbon atom and was observed at δ 168.8 (J_{Rh-C} = 54.9 Hz) in **6** and 172.0 ppm (J_{Rh-C} = 54.3 Hz) in **7**.

The tridentate coordination of the ligand in these compounds was confirmed by the molecular structure of **6**, as determined by X-ray diffraction. The crystal structure of **6** shows a distorted square planar environment at the metal center with a κ^3*C,N,N′* coordination of the lutidine-derived ligand [C1−Rh 2.029(2), N12−Rh 2.0875(17), N18−Rh 2.1579(18) Å; C1−Rh−N12 89.05(8)°, and N12−Rh−N18 78.39(7)°] (Figure 4, *top*). The pyridine ring lies at 27.6° with respect to the coordination plane, which renders a chiral helical arrangement of the tricoordinate lutidine-derived ligand, affording the enantiomers Λ and Δ shown in Figure 4 (bottom). Notably, due to the centrosymmetric space group of **6** ($P2_1/n$), both enantiomers Λ and Δ are present in the unit cell in a 1:1 molar ratio.

In sharp contrast, carbonylation of the iridium compound **2** afforded a pale orange solution from which the dicarbonyl compound [IrBr(CO)$_2$(κ*C*-^{t}BuImCH$_2$PyCH$_2$NEt$_2$)] (**8**) was isolated as a pale yellow solid in 65% yield (Scheme 2). The

https://doi.org/10.1021/acs.organomet.3c00403
Organometallics 2023, 42, 3292−3306

inequivalent carbonyl ligands of **8** were observed at δ 181.0 and 168.0 ppm in the $^{13}C\{^1H\}$ spectrum, and two strong ν(CO) stretching bands were observed at 2063 and 1980 cm^{-1} in the IR spectrum in toluene.

The ^1H NMR of **8** showed two well-separated doublets at δ 6.01 and 5.28 ppm for the protons of the Im-CH_2−Py methylene linker and a singlet at δ 3.67 ppm for the protons of the Py-CH_2−NEt_2 linker. This pattern of resonances is similar to that found in neutral bromo-complexes **1**−**3**, which also feature uncoordinated pyridine and amino fragments.

Synthesis and Structure of Cyclometalated Compounds [$MI_2\{\kappa^4C,C',N,N'$-($CH_2CMe_2ImCH_2PyCH_2NRR'$)}] (M = Rh and Ir). In order to prepare Rh(III) and Ir(III) complexes directly from the functionalized imidazolium salts, we have explored the methodology introduced by Crabtree et al. for the preparation of bis-NHC complexes.[21] Reaction of bis-imidazolium salts with dinuclear $[M(\mu\text{-Cl})(cod)]_2$ (M = Rh and Ir) compounds in the presence of potassium acetate and potassium iodide at high temperature generally leads, after long reaction times, to the formation of $[M^{III}I_2(OAc)$(bis-NHC)] (M = Rh and Ir) complexes with acetato and iodido ligands.[22]

Reaction of the imidazolium salts [^{t}BuHImCH$_2$PyCH$_2$NEt$_2$]Br and [^{t}BuHImCH$_2$PyCH$_2$NH^{t}Bu]Br with $[M(\mu\text{-Cl})(cod)]_2$ (M = Rh and Ir) in the presence of an excess of KOAc and KI in a CH_3CN/THF (1:1) mixture at 358 K for 3 days gave dark orange suspensions. The ^1H NMR of the oily residues obtained after filtering out the insoluble material and evaporating all the volatiles revealed the formation of new compounds, which were successfully separated from the reaction mixture by column chromatography. The di-iodido Rh(III) and Ir(III) cyclometalated compounds [MI_2-$\{\kappa^4C,C',N,N'$-($CH_2CMe_2ImCH_2PyCH_2NRR'$)}] (**9**−**12**) were isolated as orange or red microcrystalline solids with yields of around 10% for iridium and 25% for rhodium compounds (Scheme 3). The molecular structures of the four compounds have been determined by X-rays and are discussed below.

The new compounds, which have a tetradentate lutidine-derived polydentate ligand as a result of the activation of a C−H bond of the *t*-butyl group,[23] are stable in air and soluble in most common solvents. High-resolution ESI+ mass spectra support the stoichiometry of the compounds, in particular the presence of two iodido ligands and of an NHEt group in **10**. The metalation of the *t*-butyl group at the NHC moiety is evidenced by the presence of a ^1H resonance around δ 4.00 ppm along with the ^{13}C resonance at δ 21.5 (J_{Rh-C} = 18.6 Hz) (**9**), 4.6 (**10**), 22.7 (J_{Rh-C} = 19.5 Hz) (**11**), and 5.6 ppm (**12**) for the methylene group formed after C−H activation. Additionally, one (**9**) or two ^1H singlets (**10**−**12**) at about 1.5 ppm were observed for the two remaining methyl groups. The characteristic resonance of the carbene carbon atom was observed as a singlet at δ 146.9 (**10**) and 149.3 ppm (**12**) in the iridium compounds and as a doublet at δ 166.0 (J_{Rh-C} = 34.3 Hz) (**9**) and 169.2 ppm (J_{Rh-C} = 35.8 Hz) (**12**) in the rhodium compounds. The dealkylation of the −NEt_2 fragment in **10** was also confirmed by ^1H NMR, which showed a broad resonance at δ 4.31 assigned to the NH moiety. Dealkylation of amino ligands is uncommon, although it has been observed previously in ruthenium(II) compounds incorporating tetraethylethylenediamine ligands.[24] A possible dealkylation pathway is proposed in the Supporting Information. Finally, it is worth noting that the protons of both >CH_2 linkers were observed as two singlets in the ^1H NMR spectrum of **9** due to the existence of a symmetry plane containing the tetradentate ligand that results from the inversion of both metalacycles. However, this symmetry plane does not exist in the remaining compounds due to the presence of the −NRH group and therefore the diastereotopic >CH_2 protons appear as two doublets, AB systems, or even as two multiplets due to coupling with the proton of the neighboring NH group.

Scheme 3. Synthesis of Complexes [$MI_2\{\kappa^4C,C',N,N'$-($CH_2CMe_2ImCH_2PyCH_2NRR'$)}]

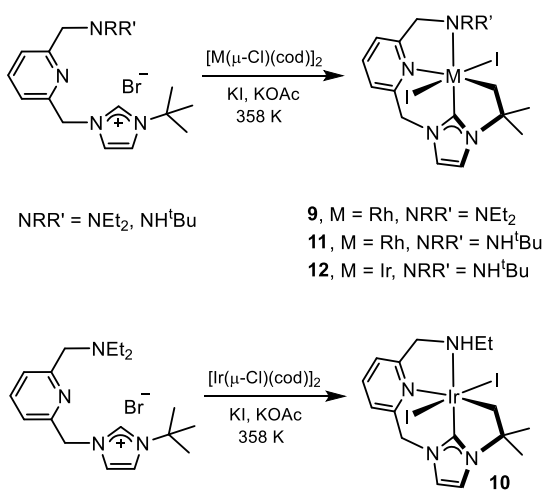

The crystal structures of **9**−**12** are shown in Figure 5 and selected bond lengths and angles are given in Table 1. All of them exhibit an octahedral environment at the metal center with two mutually trans iodido ligands [I1−M−I2 176°; M−I1/2 2.67 Å, av.]. A κ^4C,C',N,N' coordination of the lutidine-derived ligand is observed as a result of the metalation of the *tert*-butyl group along with the coordination of the amino, pyridine, and NHC moieties, affording virtually superimposable [$M\{\kappa^4C,C',N,N'$-($CH_2CMe_2ImCH_2PyCH_2NRR'$)}] fragments. Similar to **6**, the helical arrangement of the [$ImCH_2PyCH_2N$] fragment observed in **9**−**12** gives rise to Δ and Λ conformations (vide supra). Notably, as a consequence of the noncentrosymmetric space group ($P2_12_12_1$) of **9**, only the Λ enantiomer is observed in the studied crystal. On the other hand, as far as **10**−**12** are concerned, their nitrogen atom N18 is also stereogenic. Interestingly, the helical configuration of the [Im-CH_2PyCH_2N] fragment (Δ or Λ) appears to be predetermined by the configuration of the nitrogen atom (*S* or *R*), thus only one pair of enantiomers out of two possible pairs of diastereomers is observed in the solid state structures of **10**−**12**. Indeed, despite the fact that the space group of **10** is noncentrosymmetric ($P2_1$), the asymmetric unit contains a pair of independent enantiomers Λ,*R* and Δ,*S*. On the other hand, as for **11** and **12**, due to their centrosymmetric space group, namely $P2_1/c$ in both cases, enantiomers Λ,*S* and Δ,*R* are present in the crystal in a 1:1 molar ratio.

Mechanistic Studies on the Formation of Cyclometalated Compounds. Despite the low yield obtained in the preparation of cyclometalated compounds **9**−**12**, their unusual structural features lead us to investigate the mechanism of their formation by combining experimental studies with DFT calculations. For this purpose, in the first place, the formation of [$RhI_2\{\kappa^4C,C',N,N'$-

https://doi.org/10.1021/acs.organomet.3c00403
Organometallics 2023, 42, 3292−3306

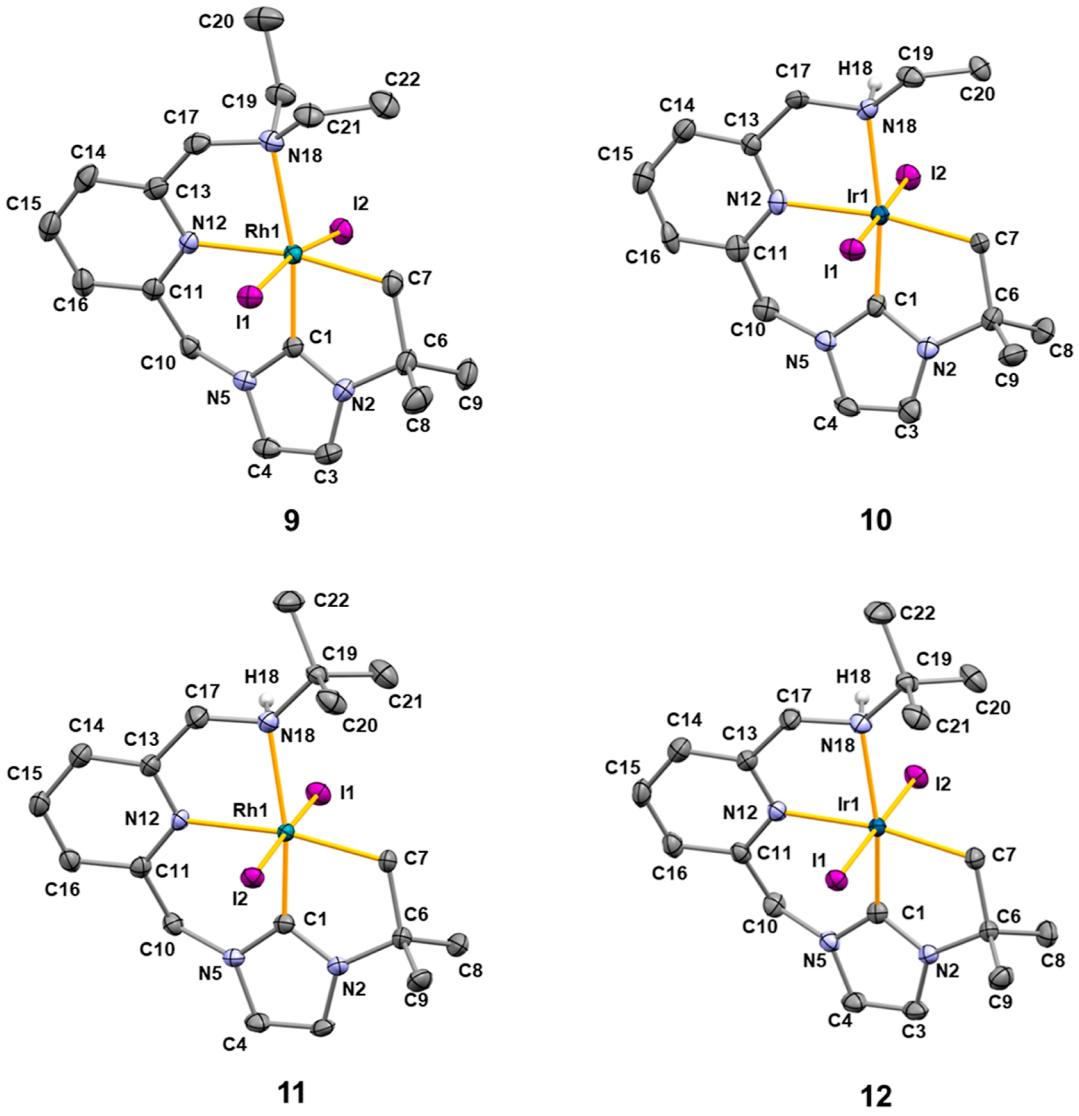

Figure 5. ORTEP views of **9**−**12**. Thermal ellipsoids are at 50% probability. For clarity, hydrogen atoms are omitted, and only the Λ,*R* enantiomer present in the asymmetric unit of **10** is shown. See Table 1 for selected bond lengths (Å) and angles (deg).

Table 1. Selected Bond Lengths (Å) and Angles (deg) of 9−12

	9	10	11	12
C1-M	1.894(3)	1.904(11)	1.893(3)	1.907(3)
C7-M	2.111(3)	2.111(10)	2.096(3)	2.113(3)
N12-M	2.127(3)	2.103(8)	2.121(2)	2.102(3)
N18-M	2.310(3)	2.205(9)	2.244(2)	2.231(3)
M−I1	2.6773(3)	2.6682(9)	2.6633(3)	2.6751(3)
M−I2	2.6699(3)	2.6635(9)	2.6701(3)	2.6693(3)
C1−M−C7	79.51(15)	79.7(4)	79.85(12)	79.35(13)
C1−M−N12	91.46(12)	92.0(4)	91.54(11)	92.25(12)
C1−M−N18	169.02(13)	171.2(4)	168.24(11)	169.01(11)
C7−M−N12	170.22(13)	171.4(4)	171.04(10)	171.15(11)
N12−M−N18	77.55(11)	79.3(3)	77.54(9)	77.65(10)
C1−M−I1	87.56(10)	90.9(3)	87.77(9)	89.74(9)
C1−M−I2	84.16(10)	90.6(3)	89.40(9)	88.81(9)
I1−M−I2	171.404(16)	178.49(3)	177.139(11)	178.382(10)

$(CH_2CMe_2ImCH_2PyCH_2NH^tBu)\}]$ (**11**) was studied starting from the imidazolium salt $[^tBuHImCH_2PyCH_2NH^tBu]Br$, the dinuclear precursor $[Rh(\mu\text{-}Cl)(cod)]_2$ (0.5 equiv), KI (4 equiv), and KOAc (8 equiv), as a model reaction to modify the experimental conditions. Thus, it was found that tetrahydrofuran is not crucial for the reaction outcome since, after 72 h at 358 K, using acetonitrile as a solvent, compound **11** was obtained in a similar yield. Furthermore, when the reaction was

https://doi.org/10.1021/acs.organomet.3c00403
Organometallics 2023, 42, 3292−3306

carried out in the absence of KI under the same conditions, [RhBr(cod)(κC-^{t}BuImCH$_2$PyCH$_2$NH^{t}Bu)] (**3**) was formed and **11** was not detected. This suggests that the presence of iodide, not only as a ligand, is essential for the formation of these M(III) compounds. Moreover, the synthesis of these cyclometalated compounds results in dark orange suspensions from which, after filtration, orange solutions and dark residues were obtained. The dark residue obtained in the synthesis of **11** was washed with water to remove any inorganic salts and then with methanol and dichloromethane to remove any soluble organic compounds. The resulting gray solid with a metallic appearance in the form of small flakes was identified as metallic rhodium by X-ray powder diffraction (XRD).

In addition, in the presence of KI and KOAc, under the same reaction conditions, the neutral complex [RhBr(cod)-(κC-^{t}BuImCH$_2$PyCH$_2$NH^{t}Bu)] (**3**) and the cationic compound [Ir(cod)(κ^{3}C,N,N′-^{t}BuImCH$_2$PyCH$_2$NEt$_2$)]PF$_6$ (**5**) also gave the cyclometalated complexes **11** and **10**, respectively, although also in low yields, suggesting that both types of compounds could be involved in the formation of the cyclometalated complexes from [M(μ-Cl)(cod)]$_2$. On this basis, the reactivity of **5** was investigated. Heating a solution of **5** in acetonitrile-d_3 at 353 K showed the gradual appearance of a new species **13** with a high-field resonance in the metal hydride region. The conversion of **5** to **13** was 86% after 8 h and was complete after 24 h. This compound, which has been identified as the cyclometalated hydrido iridium(III) compound [IrH(CH$_3$CN){κ^{4}C,C′,N,N′-(CH$_2$CMe$_2$ImCH$_2$PyCH$_2$-NEt$_2$)}]$^+$ (**13**), was isolated as a pale-yellow solid in 78% yield (Scheme 4).

Scheme 4. Synthesis of [IrH(CH$_3$CN){κ^{4}C,C′,N,N′-(CH$_2$CMe$_2$ImCH$_2$PyCH$_2$NEt$_2$)}]$^+$ (13)

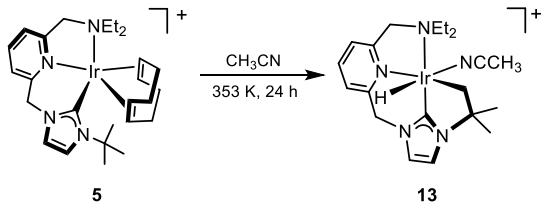

The NMR data of **13** are consistent with an unsymmetrical structure with a virtually planar cyclometalated lutidine-derived polydentate ligand. The presence of a hydrido ligand, observed as a singlet at δ −20.75 ppm, confirms the oxidative addition of a C−H bond of the *t*-butyl group to the iridium center. The remaining coordination site, trans to the hydrido ligand, should be occupied by a labile acetonitrile ligand. In contrast to **5**, the compound [IrBr(cod)(κC-^{t}BuImCH$_2$PyCH$_2$NEt$_2$)] (**2**) was recovered unchanged after heating an acetonitrile-d_3 solution at 353 K for 24 h. This result suggests that the release of the 1,5-cyclooctadiene ligand necessary for C−H activation is facilitated by the tridentate coordination of the polydentate ligand, which is prevented by the coordination of the bromido ligand in **2**.

A tentative proposal for the formation of the cyclometalated compounds [MI$_2${κ^{4}C,C′,N,N′-(CH$_2$CMe$_2$ImCH$_2$-PyCH$_2$NRR′)}] (**9**−**12**) based on the experimental observations described above is shown in Scheme 5. The deprotonation of the functionalized imidazolium salt by acetate in the presence of the dimer compounds [M(μ-Cl)(cod)]$_2$ (M = Rh and Ir) should lead to the formation of the corresponding halo-complexes **A**, which could be transformed into the cationic compounds **B** with the lutidine-derived polydentate ligand coordinated in a tridentate fashion by halide abstraction. Oxidative addition of a C−H bond from one of the methyl of the *t*-butyl group of the imidazole-2-ylidene moiety and release of the 1,5-cyclooctadiene ligand should lead to the formation of cyclometalated M(III) hydrido complexes **C** with the polydentate ligand κ^{4}C,C′,N,N′ coordinated. As the oxidative addition of the C−H bond in rhodium complexes is likely to be more energy-demanding than in iridium complexes, it cannot be ruled out that the C−H activation could also occur with the intervention of the acetate anion present in the reaction medium via a concerted metalation-deprotonation (CMD) mechanism.[25] Then, due to the likely acidic character of the hydride ligand, the following deprotonation by the acetate base should result in the formation of the square-planar M(I) intermediates [M-{κ^{4}C,C′,N,N′-(CH$_2$CMe$_2$ImCH$_2$PyCH$_2$NR$_2$)}] (**D**).[26] Finally, oxidative addition of I$_2$, formed in the reaction medium (see below), would afford the cyclometalated M(III) compounds **E** with two iodido ligands in trans disposition.

Scheme 5. Proposed Mechanism for the Formation of Cyclometalated Compounds [MI$_2${κ^{4}C,C′,N,N′-(CH$_2$CMe$_2$ImCH$_2$PyCH$_2$NRR′)}] (9−12)

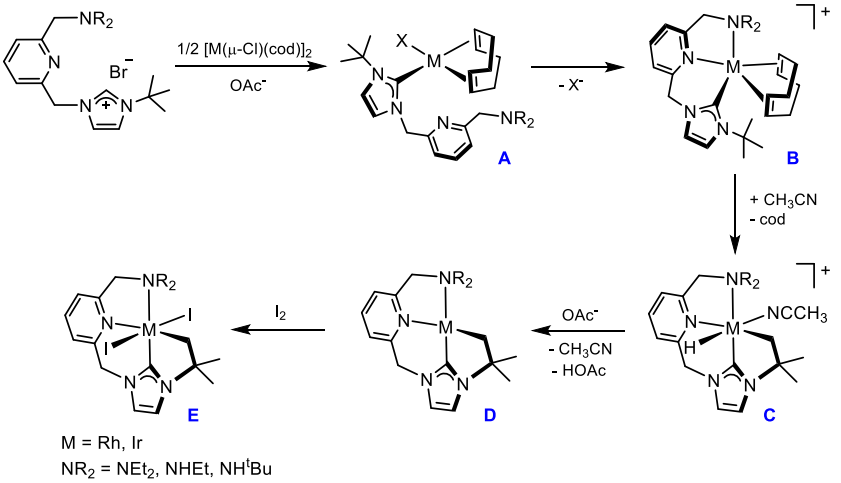

https://doi.org/10.1021/acs.organomet.3c00403
Organometallics 2023, 42, 3292−3306

The feasibility of this proposal from **C** has been investigated by a DFT study. The calculations have been carried out using the simplified platform $[M\{\kappa^4C,C',N,N'\text{-}(CH_2CMe_2ImCH_2PyCH_2NMe_2)\}]$ (M = Rh or Ir) as a model for all the complexes studied. Starting from **C**, the first step corresponds to a hydride abstraction by deprotonation with OAc^- which yields the neutral square planar species $[M\{\kappa^4C,C',N,N'\text{-}(CH_2CMe_2ImCH_2PyCH_2NMe_2)\}]$ (**D**). The DFT-optimized structure of compound **D** (M = Rh) is shown in Figure 6. This

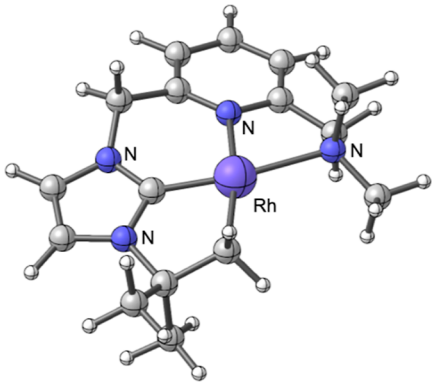

Figure 6. DFT-optimized structure of $[Rh\{\kappa^4C,C',N,N'\text{-}(CH_2CMe_2ImCH_2PyCH_2NEt_2)\}]$.

process is endergonic by only ΔG = +7.5 kcal·mol^{-1} for M = Ir and slightly exoergonic for M = Rh (ΔG = −1.6 kcal·mol^{-1}), so the deprotonation of the M(III) species by OAc^- is an easy process. This opens a pathway toward the oxidative addition of I_2 to the formed M(I) square planar species, which, as will be shown, is a highly exoergonic process (see Supporting Information and Scheme 6).

The interaction of M(I) with diiodine has been studied by scanning the distance of a diiodine molecule, I_2, from the metal center. As far as I_2 approaches the metal center, the formal oxidation of the metal atom to M(III) and the coordination of the newly formed iodide anion to M take place while the second iodine atom moves away from the complex. The evolution of Mulliken charges on both iodine atoms along the scanned coordinate shows an interesting feature as the iodine atom which dissociates develops a negative charge (ca. −0.9 e$^-$) in accordance with a free iodide anion character. All in all, this suggests an S_N2-like mechanism with the metal oxidation from M(I) to M(III), giving a cationic pentacoordinated monoiodido species $[MI\{\kappa^4C,C',N,N'\text{-}(CH_2CMe_2ImCH_2PyCH_2NMe_2)\}]^+$ (**D1**),[27] which in turn evolves to the octahedral product of the reaction **E** (see the Supporting Information). As for the reaction of **D** with I_2, neither intermediates nor TS have been located on the potential energy surface, although the formation of η^1-I_2 has been previously reported to be relevant in the oxidative addition of diiodine to rhodium or iridium complexes.[28,29]

The cationic pentacoordinate square pyramidal species $[MI\{\kappa^4C,C',N,N'\text{-}(CH_2CMe_2ImCH_2PyCH_2NMe_2)\}]^+$ (**D1**) is stabilized by 53.2 kcal·mol^{-1} for M = Ir and a similar amount in the case of M = Rh (ΔG = −54.6 kcal·mol^{-1}). Further stabilization is achieved after filling the vacant coordination position by a solvent molecule (CH_3CN), which completes the coordination sphere to give an octahedral species $[MI(CH_3CN)\{\kappa^4C,C',N,N'\text{-}(CH_2CMe_2ImCH_2PyCH_2NMe_2)\}]^+$ (**D2**) (ΔG = −12.3 kcal·mol^{-1} for M = Rh and −19.6 kcal·mol^{-1} for M = Ir). The replacement of the CH_3CN coordinated solvent by iodide to give the final M(III) neutral di-iodido compounds $[MI_2\{\kappa^4C,C',N,N'\text{-}(CH_2CMe_2ImCH_2PyCH_2NMe_2)\}]$ (**E**) leads to an additional stabilization of ΔG = −5.7 or −2.8 kcal·mol^{-1}, M = Rh or Ir, which entails a global stabilization of ΔG = −74.1 kcal·mol^{-1} for Rh or −68.1 kcal·mol^{-1} for Ir relative to the starting hydrido compounds (**C**). According to Hammond's postulate,[30] given the high exergonicity, the activation barrier must be very low, and, in fact, no TS has

Scheme 6. Gibbs Energy Profile (ΔG in kcal mol^{-1}) for the Transformation of C into E (M = Rh, blue line; M = Ir, red line)

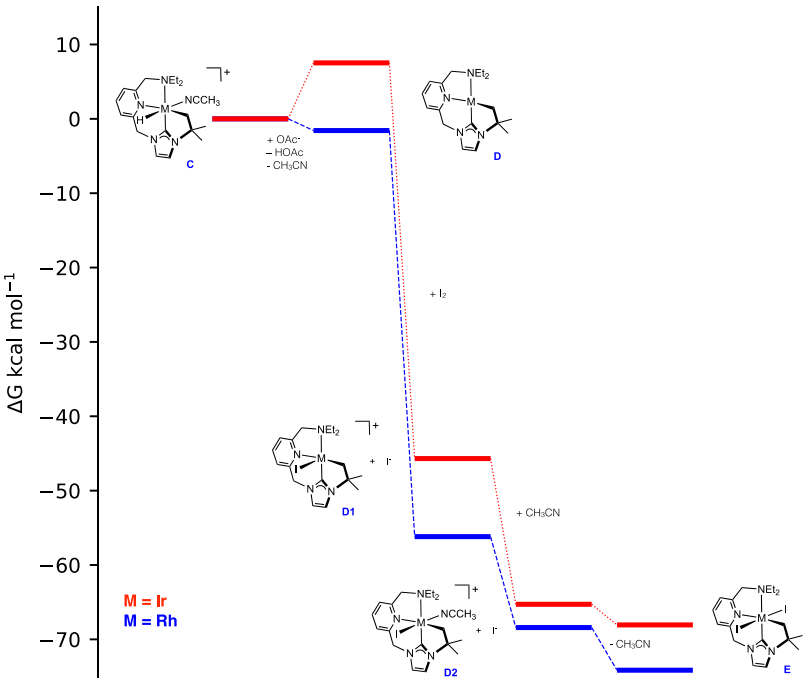

https://doi.org/10.1021/acs.organomet.3c00403
Organometallics 2023, 42, 3292−3306

been found at this level of calculation. The energy profile for the transformation of **C** into **E** is shown in Scheme 6.

Unfortunately, attempts to synthesize [Ir{κ^4*C*,*C*′,*N*,*N*′-($CH_2CMe_2ImCH_2PyCH_2NEt_2$)}] by deprotonation of **13** with a strong base were unsuccessful. The addition of KHMDS (1.2 equiv) to a solution of **13** in acetonitrile at 253 K, followed by slow warming to room temperature, gave a brown solid, which turned out to be a mixture of unidentified compounds. We hypothesized that competitive deprotonation of the acidic methylene arms of the ligand prevents the synthesis of the target compound.[10c,13b,18b] In this regard, DFT calculations have shown that the deprotonation of the Im-CH_2−Py arm in **13** by acetate is also an endergonic process by ΔG = +8.15 kcal mol^{-1}, only +0.65 kcal mol^{-1} more endergonic than the deprotonation of the hydrido ligand (see above). Similarly, attempts to synthesize complex [IrI_2{κ^4*C*,*C*′,*N*,*N*′-($CH_2CMe_2ImCH_2PyCH_2NEt_2$)}] from **13** by a sequential reaction with OAc^- and diiodine failed and resulted in a mixture of two main compounds, which could neither be separated nor characterized. This result suggests that the formation of diiodine probably has to occur slowly to avoid side reactions, which is consistent with the required long reaction time.

The mechanism of I_2 formation, which is proposed to be involved in the formation of the cyclometalated compounds, is controversial. Previous reports on the synthesis of bis-NHC rhodium(III) and iridium(III) compounds of general formula [MI_2(OAc)(bis-NHC)] point to the participation of I_2, which is thought to form by slow oxidation of iodide by adventitious O_2(*g*) in the reaction medium.[31] In fact, improved yields were obtained in the synthesis of [RhI_2(OAc)(bis-NHC)] complexes when the reactions were carried out in the presence of air or in aerated solvents.[32] However, no oxygen effect was observed in the synthesis of related Ir(III) complexes, which were also isolated in modest yields.[33] In our case, the yield of **11** did not improve when the reaction was carried out under air, although the formation of unidentified species was observed in the ^{1}H NMR of the reaction crude.

On the other hand, the formation of metallic rhodium in the synthesis of **11** suggests that a disproportionation process may be involved in the formation of molecular diiodine. First, thermal disproportionation of the M(I) square-planar [M^I{κ^4*C*,*C*′,*N*,*N*′-($CH_2CMe_2ImCH_2PyCH_2NR_2$)} (**D**) species could yield M(0) and cationic M(II) species [M^{II}{κ^4*C*,*C*′,*N*,*N*′-($CH_2CMe_2ImCH_2PyCH_2NR_2$)}]$^+$. Reaction of the M(II) species with iodide (I^-) would regenerate the M(I) intermediate with the formation of an iodo radical (I•) that could dimerize rendering I_2. In this regard, it is worth noting that the spontaneous disproportionation of a neutral rhodium(I) bisoxazolinate compound to a rhodium(II) species and metallic rhodium has been reported.[34]

Monitoring of the formation of **11** by ^{1}H NMR analysis of reaction aliquots exclusively showed the presence of [Rh(μ-Cl)(cod)]$_2$, imidazolium salt, the cyclometalated product **11**, and unidentified minor species, but there were no reaction intermediates (see Supporting Information). In agreement with the formation of metallic rhodium, the rhodium dimer was completely, consumed whereas part of the imidazolium salt remains unreacted (vide infra). The formation of metallic rhodium is partly responsible for the low yield attained in the synthesis of the cyclometalated compounds. According to the stoichiometry of the proposed disproportionation reaction, the maximum attainable yield is 33%. However, another factor that may contribute to the observed poor yield could be the instability of the intermediates under the reaction conditions, in particular, the proposed cyclometalated square planar intermediate **D**. Finally, the ratio of **11** to imidazolium salt after 72 h is roughly 3:2, confirming the loss of imidazolium salt likely as an insoluble rhodium species.

CONCLUSIONS

The rhodium and iridium coordination chemistry of lutidine-based ligands with NHC and amino side-donor functions has been explored. Rh(I) and Ir(I) complexes [MBr(cod)(κ*C*-^{t}BuIm$CH_2PyCH_2NR_2$)], with the ligand exclusively coordinated through the NHC moiety, are accessible via deprotonation of the functionalized imidazolium salts, [^{t}BuHIm$CH_2PyCH_2NR_2$]Br, by the bridging methoxo ligands of the dinuclear complexes [M(μ-OMe)(cod)]$_2$. Abstraction of the bromido ligand induces the coordination of both pyridine and amino fragments to afford cationic pentacoordinated complexes [M(cod)(κ^3*C*,*N*,*N*′-^{t}Bu$ImCH_2PyCH_2NR_2$)]$^+$ with a distorted trigonal bypiramidal structure. The outcome of the carbonylation of [MBr(cod)(κ*C*-^{t}Bu$ImCH_2PyCH_2NR_2$)] has been found to be dependent on the metal center. Carbonylation of the rhodium complexes results in the formation of unusual cationic complexes [Rh(CO)(κ^3*C*,*N*,*N*′-^{t}Bu$ImCH_2PyCH_2NR_2$)]$^+$ with a genuine pincer structure and a single carbonyl ligand. In contrast, carbonylation of the iridium compound results in the formation of the neutral dicarbonyl complex [$IrBr(CO)_2$(κ*C*-^{t}Bu$ImCH_2PyCH_2NR_2$)].

The straightforward metalation of imidazolium salts [^{t}BuHIm$CH_2PyCH_2NR_2$]Br with the dinuclear compounds [M(μ-Cl)(cod)]$_2$ (M = Rh and Ir) in the presence of potassium acetate and potassium iodide provides access to unprecedented di-iodido M(III) cyclometalated compounds [MI_2{κ^4*C*,*C*′,*N*,*N*′-($CH_2CMe_2ImCH_2PyCH_2NR_2$)}], albeit in low yields, as a result of the metalation of the *tert*-butyl group. Investigation of the reaction mechanism has shown that compound [Ir(cod)(κ^3*C*,*N*,*N*′-^{t}Bu$ImCH_2PyCH_2NEt_2$)]$^+$, a precursor for the synthesis of the di-iodido cyclometalated compound, easily transforms under thermal conditions into the cyclometalated Ir(III) hydrido compound [IrH(CD_3CN)-{κ^4*C*,*C*′,*N*,*N*′-($CH_2CMe_2ImCH_2PyCH_2NEt_2$)}]$^+$. DFT calculations have shown that deprotonation of these hydrido complexes by acetate to afford the square-planar cyclometalated M(I) [M{κ^4*C*,*C*′,*N*,*N*′-(CH_2CMe_2-$ImCH_2PyCH_2NR_2$)}], followed by oxidative addition of I_2, formed in the reaction medium, is a feasible route to the di-iodido M(III) cyclometalated compounds. Experimental evidence rules out the participation of dioxygen in the formation of diiodine. The low yield attained in the synthesis of these compounds and the formation of metallic rhodium suggest that a disproportionation process may be involved in the formation of diiodine.

EXPERIMENTAL SECTION

General Considerations. All reactions were carried out with rigorous exclusion of air using Schlenk-tube techniques or a glovebox. Organic solvents were dried by standard methods and distilled under argon prior to use or obtained oxygen- and water-free from a solvent purification system (Innovative Technologies). The starting materials [Rh(μ-Cl)(cod)]$_2$,[35] [Ir(μ-Cl)(cod)]$_2$,[36] and [M(μ-OMe)(cod)]$_2$ (M = Rh and Ir)[37] were prepared as previously described in the literature. The imidazolium salts [^{t}BuHIm$CH_2PyCH_2NEt_2$]Br and [^{t}BuHIm$CH_2PyCH_2NH^tBu$]Br were prepared following the proce-

https://doi.org/10.1021/acs.organomet.3c00403
Organometallics 2023, 42, 3292−3306

dure recently described by us.[12] Deuterated solvents (Euriso-top) $CDCl_3$, CD_2Cl_2, C_6D_6, and CD_3CN were dried using activated molecular sieves.

Scientific Equipment. C, H, and N analyses were carried out in a PerkinElmer 2400 Series II CHNS/O analyzer. Infrared spectra were recorded on a 100 FTIR-PerkinElmer Spectrophotometer equipped with a Universal Attenuated Total Reflectance (UATR) accessory, which allows the observation of the electromagnetic spectrum over the 4000−250 cm^{-1} region. ^1H and $^{13}C\{^1H\}$ NMR spectra were recorded on a Bruker Avance 300 (300.1278 MHz) or Bruker Avance 400 (400.130 MHz). Chemical shifts are reported in ppm relative to tetramethylsilane, and coupling constants (J) are given in Hertz (Hz). Spectral assignments were achieved by a combination of $^1H-^1H$ COSY, ^{13}C APT, $^1H-^{13}C$ HSQC, and $^1H-^{13}C$ HMBC experiments. High-resolution electrospray ionization mass spectra (HRMS-ESI) were recorded using a Bruker MicroToF-Q equipped with an API-ESI source and a Q-ToF mass analyzer, which leads to a maximum error in the measurement of 5 ppm, using sodium formate as a reference. Conductivities were measured in ca. 5×10^{-4} M nitromethane solutions of the complexes using a Philips PW 9501/01 conductimeter.

Synthesis of [RhBr(cod)(κC-^{t}BuImCH$_2$PyCH$_2$NEt$_2$)] (1). $[Rh(\mu\text{-}OMe)(cod)]_2$ (127 mg, 0.262 mmol) was added to a solution of $[^t$BuHImCH$_2$PyCH$_2$NEt$_2$]Br (200 mg, 0.524 mmol) in dichloromethane (5 mL) and stirred for 15 h at room temperature. The resulting yellow solution was brought to dryness under a vacuum to give an oily residue that was disaggregated by stirring with cold pentane. The solid was filtered, washed with pentane (2 × 5 mL), and dried under vacuum. Yield: 267 mg, 86% (pale yellow solid). Anal. Calcd for $C_{26}H_{40}BrN_4Rh$: C, 52.80; H, 6.82; N, 9.47. Found: C, 52.39; H, 6.44; N, 9.82. HRMS (ESI+, MeOH, m/z): calcd for $C_{26}H_{40}BrN_4Rh$, 590.1491 [M]; found, 591.1564 $[M-H]^+$. ^1H NMR (300 MHz, $CDCl_3$, 298 K): δ 7.63 (t, J_{H-H} = 7.7 Hz, 1H, H_p Py), 7.45−7.36 (m, 2H, H_m Py), 7.01 (d, J_{H-H} = 2.1 Hz, 1H, =CH Im), 6.84 (d, J_{H-H} = 2.0 Hz, 1H, =CH Im), 6.73 (d, J_{H-H} = 14.9 Hz, 1H, CH_2Im), 5.91 (d, J_{H-H} = 14.8 Hz, 1H, CH_2Im), 5.09−5.02 (br, 2H, =CH cod, trans NHC), 3.74 (s, 2H, CH_2NEt_2), 3.48 (m, 1H, =CH cod, trans Br), 3.34 (m, 1H,=CH cod, trans Br), 2.59 (q, J_{H-H} = 7.1 Hz, 4H, CH_2 Et), 2.47−2.19 (m, 4H, > CH_2 cod), 1.98 (s, 9H, ^{t}Bu), 1.90−1.66 (m, 4H, > CH_2 cod), 1.06 (t, J_{H-H} = 7.1 Hz, 6H, CH_3 Et). $^{13}C\{^1H\}$ NMR (75 MHz, $CDCl_3$, 298 K): δ 180.9 (d, J_{C-Rh} = 49.7 Hz, C_{NCN}), 160.3, 155.9 (C_o Py), 137.5 (C_p Py), 122.2, 121.7 (C_m Py), 120.5, 120.3 (=CH Im), 96.2 (d, J_{C-Rh} = 7.5 Hz, =CH cod, trans NHC), 94.0 (d, J_{C-Rh} = 7.2 Hz, =CH cod, trans NHC), 71.5 (d, J_{C-Rh} = 15.4 Hz, =CH cod, trans Br), 68.2 (d, J_{C-Rh} = 14.3 Hz, =CH cod, trans Br), 59.5 (CH_2NEt_2), 58.6 (C ^{t}Bu), 58.5 (CH_2Im), 47.5 (CH_2 Et), 33.4 (>CH_2 cod), 32.4 (CH_3 ^{t}Bu), 31.5, 29.9, 28.6 (>CH_2 cod), 12.1 (CH_3 Et).

Synthesis of [IrBr(cod)(κC-^{t}BuImCH$_2$PyCH$_2$NEt$_2$)] (2). The compound was prepared from $[^t$BuHImCH$_2$PyCH$_2$NEt$_2$]Br (200 mg, 0.524 mmol) and $[Ir(\mu\text{-}OMe)(cod)]_2$ (174 mg, 0.262 mmol) following the procedure described above for **1**. Yield: 330 mg, 93% (dark yellow solid). Anal. Calcd for $C_{26}H_{40}BrN_4Ir$: C, 45.87; H, 5.92; N, 8.23. Found: C, 45.47; H, 5.74; N, 7.95. HRMS (ESI+, MeOH, m/z): calcd for $C_{26}H_{40}BrN_4Ir$, 680.2065 [M]; found, 681.2123 $[M+H]^+$. ^1H NMR (300 MHz, $CDCl_3$, 298 K): δ 7.62 (t, J_{H-H} = 7.7 Hz, 1H, H_p Py), 7.39 (d, J_{H-H} = 7.6 Hz, 1H, H_m Py), 7.34 (d, J_{H-H} = 7.6 Hz, 1H, H_m Py), 7.03 (d, J_{H-H} = 2.1 Hz, 1H, =CH Im), 6.89 (d, J_{H-H} = 2.1, 1H, =CH Im), 6.68 (d, J_{H-H} = 14.8 Hz, 1H, CH_2Im), 5.73 (d, J_{H-H} = 14.8 Hz, 1H, CH_2Im), 4.64−4.48 (m, 2H, =CH cod, trans NHC), 3.73 (s, 2H, CH_2NEt_2), 2.96 (br, 2H, =CH cod, trans Br), 2.59 (q, J_{H-H} = 7.1 Hz, 4H, CH_2 Et), 2.30−2.09 (m, 4H, > CH_2 cod), 1.90 (s, 9H, ^{t}Bu), 1.77−1.43 (m, 4H, > CH_2 cod), 1.06 (t, 6H, J_{H-H} = 7.1 Hz, CH_3 Et). $^{13}C\{^1H\}$ NMR (75 MHz, $CDCl_3$, 298 K): δ 180.0 (C_{NCN}), 160.2, 155.8 (C_o Py), 137.6 (C_p Py), 122.1, 121.3 (C_m Py), 120.0, 119.9 (=CH Im), 82.5, 80.2 (=CH cod, trans NHC), 59.6 (CH_2NEt_2), 59.0 (C ^{t}Bu), 58.5 (CH_2Im), 53.8, 51.3 (=CH cod, trans Br), 47.5 (CH_2 Et), 33.7, 33.0 (>CH_2 cod), 32.8 (CH_3 ^{t}Bu), 29.7, 29.5 (>CH_2 cod), 12.1 (CH_3 Et).

Synthesis of [RhBr(cod)(κC-^{t}BuImCH$_2$PyCH$_2$NH^{t}Bu)] (3). $[Rh(\mu\text{-}Cl)(cod)]_2$ (129 mg, 0.262 mmol) was added to a solution of NaH (25 mg, 1.042 mmol) in ethanol (10 mL). The suspension was placed in an ultrasonic bath for 5 min and stirred at room temperature for 30 min. $[^t$BuHImCH$_2$PyCH$_2$NH^{t}Bu]Br (200 mg, 0.524 mmol) was added over the resulting yellow suspension and stirred for 2 h at room temperature. The suspension was brought to dryness under a vacuum, dissolved in dichloromethane (10 mL), filtered, and the solid was washed with dichloromethane (2 × 5 mL). To the obtained solution, KBr (624 mg, 5.240 mmol) was added in excess and stirred at room temperature for 17 h. The suspension was filtered, and the solid was washed with dichloromethane (2 × 5 mL). The solution was brought to dryness under a vacuum, and the resulting oily residue was disintegrated at a low temperature (195 K). The dark yellow solid was filtered off, washed with cold distilled water (2 × 5 mL), and dried under a vacuum for a long time. Yield: 186 mg, 60% (yellow solid). Anal. Calcd for $C_{26}H_{40}BrN_4Rh$: C, 52.80; H, 6.82; N, 9.47. Found: C, 52.67; H, 6.62; N, 9.24. HRMS (ESI+, MeOH, m/z): calcd for $C_{26}H_{40}BrN_4Rh$, 590.1491 [M]; found, 511.2259 $[M-Br]^+$. ^1H NMR (300 MHz, $CDCl_3$, 298 K): δ 7.59 (t, J_{H-H} = 7.7 Hz, 1H, H_p Py), 7.35 (d, J_{H-H} = 7.7 Hz, 1H, H_m Py), 7.21 (d, J_{H-H} = 7.6 Hz, 1H, H_m Py), 6.99 (d, J_{H-H} = 2.1 Hz, 1H, =CH Im), 6.82 (d, J_{H-H} = 2.1 Hz, 1H, =CH Im), 6.58 (d, J_{H-H} = 15.0 Hz, 1H, CH_2Im), 6.09 (d, J_{H-H} = 15.0 Hz, 1H, CH_2Im), 4.94 (br, 2H, =CH cod, trans NHC), 3.85 (s, 2H, CH_2NH^tBu), 3.41 (m, 1H, =CH cod, trans Br), 3.29 (m, 1H, =CH cod, trans Br), 2.47−2.20 (m, 4H, > CH_2 cod), 1.97 (s, 9H, ^{t}BuIm), 1.92−1.69 (m, 4H, > CH_2 cod), 1.33 (s, 1H, NH), 1.15 (s, 9H, ^{t}BuNH). $^{13}C\{^1H\}$ NMR (75 MHz, $CDCl_3$, 298 K): δ 181.3 (d, J_{C-Rh} = 50.6 Hz, C_{NCN}), 159.9, 156.0 (C_o Py), 137.6 (C_p Py), 121.5, 121.3 (C_m Py), 120.5, 120.1 (=CCH Im), 96.8 (d, J_{C-Rh} = 7.6 Hz, =CH cod, trans NHC), 94.4 (d, J_{C-Rh} = 7.3 Hz, =CH cod, trans NHC), 70.4 (d, J_{C-Rh} = 15.3 Hz, =CH cod, trans Br), 67.2 (d, J_{C-Rh} = 14.4 Hz, =CH cod, trans Br), 58.5 (C ^{t}BuIm), 58.1 (CH_2Im), 50.5 (C ^{t}BuNH), 48.2 (CH_2NH^tBu), 33.3 (>CH_2 cod), 32.4 (CH_3 ^{t}BuIm), 31.9, 29.3 (>CH_2 cod), 29.1 (CH_3 ^{t}BuNH), 28.5 (>CH_2 cod).

Synthesis of [Rh(cod)(κ^{3}C,N,N′-^{t}BuImCH$_2$PyCH$_2$NEt$_2$)]PF$_6$ (4). $AgPF_6$ (85.0 mg, 0.338 mmol) was added to a solution of [RhBr(cod)(κC-^{t}BuImCH$_2$PyCH$_2$NEt$_2$)] (**1**) (200 mg, 0.338 mmol) in dichloromethane (5 mL). The suspension was stirred at room temperature in the absence of light for 30 min, filtered through Celite to remove the silver bromide formed, and washed with dichloromethane (2 × 5 mL). The solution was brought to dryness under a vacuum to give an oily residue, which was disaggregated by stirring with cold diethyl ether. The solid was filtered, washed with diethyl ether (2 × 5 mL), and dried under vacuum. Yield: 155 mg, 70% (yellow solid). Anal. Calcd for $C_{26}H_{40}F_6N_4PRh$: C, 47.57; H, 6.14; N, 8.53. Found: C, 47.18; H, 6.24; N, 8.44. HRMS (ESI+, MeOH, m/z): calcd for $C_{26}H_{40}N_4Rh$, 511.2308; found, 511.2303 $[M]^+$. Λ_M (nitromethane, 5.0×10^{-4} M) = 81 $\Omega^{-1}cm^2$ mol^{-1}. ^1H NMR (300 MHz, CD_3CN, 298 K): δ 7.76 (t, J_{H-H} = 7.9 Hz, 1H, H_p Py), 7.46 (d, J_{H-H} = 7.4 Hz, 1H, H_m Py), 7.30 (d, J_{H-H} = 1.8 Hz, 1H, =CH Im), 7.25 (d, J_{H-H} = 2.0 Hz, 1H, =CH Im), 7.15 (d, J_{H-H} = 7.5 Hz, 1H, H_m Py), 6.27 (d, J_{H-H} = 15.4 Hz, 1H, CH_2Im), 5.89 (d, J_{H-H} = 15.4 Hz, 1H, CH_2Im), 4.80−4.56 (m, 2H, =CH cod), 4.03−3.94 (br, 2H, =CH cod)), 3.72 (ABq, δ_A = 3.76, δ_B = 3.67 J_{A-B} = 5.0 Hz, 2H, CH_2NEt_2), 2.58−2.46 (m, 4H, CH_2 Et), 2.45−2.36 (m, 4H, >CH_2 cod), 1.88 (s, 9H, ^{t}Bu), 1.83−1.71 (m, 4H, > CH_2 cod), 0.98 (t, J_{H-H} = 7.2 Hz, 6H, CH_3 Et). $^{31}P\{^1H\}$ NMR (121.4 MHz, CD_3CN, 298 K): δ −144.5 (sept). $^{13}C\{^1H\}$ NMR (75 MHz, CD_3CN, 298 K): δ 172.7 (C_{NCN}), 162.3 155.0 (C_o Py), 134.5 (C_p Py), 121.6, 121.5 (C_m Py), 120.0, 118.1 (=CH Im), 79.9, 73.7 (=CH cod), 62.5 (CH_2NEt_2), 59.6 (C ^{t}Bu), 57.5, 54.1 (=CH cod), 51.2 (CH_2Im), 46.7 (CH_2 Et), 31.5 (>CH_2 cod), 31.1 (CH_3 ^{t}Bu), 30.6, 28.7, 27.6 (>CH_2 cod), 10.5 (CH_3 Et).

Synthesis of [Ir(cod)(κ^{3}C,N,N′-^{t}BuImCH$_2$PyCH$_2$NEt$_2$)]PF$_6$ (5). The compound was prepared from [IrBr(cod)-(κC-^{t}BuImCH$_2$PyCH$_2$NEt$_2$)] (**2**) (200 mg, 0.294 mmol) and $AgPF_6$ (74.0 mg, 0.294 mmol) following the procedure described above for **4**. Yield: 164 mg, 75% (pale brown solid). Anal. Calcd for

https://doi.org/10.1021/acs.organomet.3c00403
Organometallics 2023, 42, 3292−3306

$C_{26}H_{40}F_6N_4PIr$: C, 41.87; H, 5.41; N, 7.51. Found: C, 41.21; H, 5.35; N, 7.76. HRMS (ESI+, MeOH, m/z): calcd for $C_{26}H_{40}N_4Ir$, 601.2883; found, 601.2858 $[M]^+$. Λ_M (nitromethane, 5.0×10^{-4} M) = 90 $\Omega^{-1}cm^2$ mol^{-1}. ^1H NMR (300 MHz, $CDCl_3$, 298 K): δ 7.87−7.78 (m, 2H, H_m y H_p Py), 7.76 (d, J_{H-H} = 6.7 Hz, 1H, H_m Py), 7.50 (d, J_{H-H} = 2.0 Hz, 1H, =CH Im), 7.04 (d, J_{H-H} = 2.0 Hz, 1H, =CH Im), 5.99 (d, J_{H-H} = 14.9 Hz, 1H, CH_2Im), 5.65 (d, J_{H-H} = 14.9 Hz, 1H, CH_2Im), 4.18 (d, J_{H-H} = 15.5 Hz, 1H, CH_2NEt_2), 3.94−3.70 (m, 3H, =CH cod), 3.80 (d, J_{H-H} = 15.5 Hz, 1H, CH_2NEt_2), 3.56 (m, 1H, =CH cod), 2.51−2.32 (m, 4H, CH_2 Et), 2.17−1.93 (m, 4H, > CH_2 cod), 1.68 (s, 9H, ^{t}Bu), 1.63−1.47 (m, 4H, > CH_2 cod), 0.98 (t, J_{H-H} = 7.1 Hz, 6H, CH_3 Et). $^{31}P\{^1H\}$ NMR (121.4 MHz, $CDCl_3$, 298 K): δ −144.7 (sept). $^{13}C\{^1H\}$ NMR (75 MHz, $CDCl_3$, 298 K): δ 172.3 (C_{NCN}), 162.6, 153.9 (C_o Py), 139.5 (C_p Py), 125.0, 124.9 (C_m Py), 123.0, 118.9 (=CH Im), 84.6, 75.2 (=CH cod), 61.8 (CH_2NEt_2), 60.1 (=CH cod), 58.3 (C ^{t}Bu), 56.48 (CH_2Im), 56.11 (=CH cod), 47.7 (CH_2 Et), 33,6 (>CH_2 cod), 32.5 (CH_3 ^{t}Bu), 31.6, 29.9, 29.1 (>CH_2 cod), 12.0 (CH_3 Et).

Synthesis of [Rh(CO)(κ³*C*,*N*,*N*′-^{t}BuImCH$_2$PyCH$_2$NEt$_2$)]Br (6). CO(g) was bubbled through a solution of [RhBr(cod)-(κ*C*-^{t}BuImCH$_2$PyCH$_2$NEt$_2$)] (**1**) (100 mg, 0.169 mmol) in toluene (5 mL) for 30 min. The resulting yellow solution was brought to dryness under vacuum to give an oily residue, which was disaggregated by stirring with cold diethyl ether. The yellow solid was filtered, washed with diethyl ether (2 × 5 mL), and dried under a vacuum. Yield: 60 mg, 69%. Anal. Calcd for $C_{19}H_{28}BrN_4ORh$: C, 44.64; H, 5.52; N, 10.96. Found: C, 44.87; H, 5.50; N, 10.68. HRMS (ESI+, MeOH, m/z): calcd for $C_{19}H_{28}N_4ORh$: 431.1318; found, 431.1302 $[M]^+$, 403.1344 $[M - CO]^+$. FTIR-ATR (cm^{-1}): 1946 (ν_{CO}). Λ_M (nitromethane, 5.0×10^{-4} M) = 77.6 $\Omega^{-1}cm^2$ mol^{-1}. ^1H NMR (300 MHz, $CDCl_3$, 298 K): δ 8.19 (d, J_{H-H} = 7.5 Hz, 1H, H_m Py), 7.90 (t, J_{H-H} = 7.8 Hz, 1H, H_p Py), 7.85 (d, J_{H-H} = 2.1 Hz, 1H, =CH Im), 7.68 (d, J_{H-H} = 7.9 Hz, 1H, H_m Py), 7.11 (d, J_{H-H} = 2.1 Hz, 1H, =CH Im), 5.77 (s, 2H, CH_2Im), 4.28 (s, 2H, CH_2NEt_2), 3.15−2.96 (m, 2H, $N(CH_2CH_3)_2$), 2.92−2.64 (m, 2H, CH_2 Et), 1.87 (s, 9H, ^{t}Bu), 1.47 (t, J_{H-H} = 7.1 Hz, 6H, CH_3 Et). $^{13}C\{^1H\}$ NMR (75 MHz, $CDCl_3$, 298 K): δ 193.2 (d, J_{C-Rh} = 81.2 Hz, CO), 168.8 (d, J_{C-Rh} = 54.9 Hz, C_{NCN}), 160.5, 154.6 (C_o Py), 140.9 (C_p Py), 124.3 (C_m Py), 122.9 (=CH Im, C_m Py), 119.0 (=CH Im), 63.6 (CH_2NEt_2), 59.1 (C ^{t}Bu), 54.6 (CH_2Im, CH_2 Et), 32.5 (CH_3 ^{t}Bu), 12.5 (CH_3 Et).

Synthesis of [Rh(CO)(κ³*C*,*N*,*N*′-^{t}BuImCH$_2$PyCH$_2$NH^{t}Bu)]Br (7). CO(g) was bubbled through a solution of [RhBr(cod)-(κ*C*-^{t}BuImCH$_2$PyCH$_2$NH^{t}Bu)] (**3**) (100 mg, 0.169 mmol) in toluene (5 mL) for 30 min to give a dark suspension. The suspension was filtered, and the black solid was washed with toluene (2 × 3 mL). The resulting yellow solution was brought to dryness in vacuo to give an oily residue that was disaggregated by stirring with cold pentane. The yellow solid was filtered, washed with pentane (2 × 5 mL), and dried under a vacuum. Yield: 52 mg, 60%. Anal. Calcd for $C_{19}H_{28}BrN_4ORh$: C, 44.64; H, 5.52; N, 10.96. Found: C, 44.52; H, 5.14; N, 11.23. HRMS (ESI+, MeOH, m/z): calcd for $C_{19}H_{28}N_4ORh$: 431.1318; found, 431.1326 $[M]^+$, 403.1374 $[M - CO]^+$. FTIR-ATR (cm^{-1}): 1947 (ν_{CO}). Λ_M (nitromethane, 5.0×10^{-4} M) = 60.7 $\Omega^{-1}cm^2$ mol^{-1}. ^1H NMR (400 MHz, CD_3CN, 298 K): δ 7.94 (t, J_{H-H} = 7.8 Hz, 1H, H_p Py), 7.60−7.51 (m, 2H, H_m Py, H_m Py), 7.37 (d, J_{H-H} = 2.2 Hz, 1H, =CH Im), 7.31 (d, J_{H-H} = 2.1 Hz, 1H, =CH Im), 5.45 (br, 1H, NH), 5.37 (br, 2H, CH_2Im), 4.38 (br, 2H, CH_2NH^tBu), 1.87 (s, 9H, ^{t}BuIm), 1.19 (s, 9H, ^{t}BuNH). $^{13}C\{^1H\}$ NMR (100.6 MHz, CD_3CN, 298 K): δ 195.4 (d, J_{Rh-C} = 79.8 Hz, CO), 172.0 (d, J_{Rh-C} = 54.3 Hz, C_{CNC}), 164.8, 154.5 (C_o Py), 141.7 (C_p Py), 123.1, 122.5 (C_m Py), 122.4, 120.6 (=CH Im), 60.1 (C ^{t}BuIm), 58.5 (C ^{t}BuNH), 55.7 (CH_2Im), 53.6 (CH_2NH^tBu), 32.5 (CH_3 ^{t}BuIm), 29.5 (CH_3 ^{t}BuNH).

Synthesis of [IrBr(CO)$_2$(κ*C*-^{t}BuImCH$_2$PyCH$_2$NEt$_2$)] (8). Carbon monoxide was bubbled through a solution of [IrBr(cod)-(κ*C*-^{t}BuImCH$_2$PyCH$_2$NEt$_2$)] (**2**) (100 mg, 0.147 mmol) in tetrahydrofuran (5 mL) for 5 min at room temperature to give a pale orange solution. The solvent was removed under a vacuum, and the residue washed with cold pentane (3 × 5 mL) and dried under a vacuum to give a pale-yellow solid. Yield: 60 mg, 65%. HRMS (ESI+, CH_3CN, m/z): calcd for $C_{20}H_{28}BrN_4O_2Ir$: 628.1025; found: 521.1901 $[M - Br - CO]^+$. TFIR (toluene, cm^{-1}): 2063, 1980 cm^{-1} (ν_{CO}). Λ_M (acetone, 5.0×10^{-4} M) = 19.1 $\Omega^{-1}cm^2$ mol^{-1}. ^1H NMR (400 MHz, C_6D_6, 298 K): δ 7.32 and 7.08 (both d, J_{H-H} = 7.2, 2H, H_m Py), 7.12 (t, J_{H-H} = 7.2, 1H, H_p Py), 6.63 (d, J_{H-H} = 2.0 Hz, 1H, =CH Im), 6.32 (d, J_{H-H} = 2.0 Hz, 1H, =CH Im), 6.01 (d, J_{H-H} = 15.1 Hz, 1H, CH_2Im), 5.28 (d, J_{H-H} = 15.1 Hz, 1H, CH_2Im), 3.67 (s, 2H, CH_2NEt_2), 2.38 (q, J_{H-H} = 7.2, 4H, CH_2 Et), 1.39 (s, 9H, ^{t}Bu), 0.90 (t, J_{H-H} = 7.2, 6H, CH_3 Et). $^{13}C\{^1H\}$ NMR (100.6 MHz, C_6D_6, 298 K): δ 181.4 and 168.8 (CO), 172.5 (C_{NCN}), 161.8 and 154.6 (C_q Py), 1367.1 (C_p Py), 122.0 and 121.4 (C_m Py), 121.4 and 119.5 (=CH Im), 60.0 (CH_2NEt_2), 58.2 (CH_2Im), 47.7 (CH_2Et), 32.1 (^{t}Bu), 12.4 (CH_3 Et).

Synthesis of Compounds [MI$_2${κ⁴*C*,*C*′,*N*,*N*′-(CH$_2$CMe$_2$ImCH$_2$PyCH$_2$NRR′)}] (M = Rh and Ir). *General Method.* KI and KOAc were added to a solution of $[M(\mu\text{-Cl})(cod)]_2$ (M = Rh and Ir) and [^{t}BuHImCH$_2$PyCH$_2$L]Br (L = NEt_2 and NH^tBu) in an acetonitrile-tetrahydrofuran mixture (10 mL, 1:1). The mixture was stirred for 3 days in a reinforced glass reactor at 358 K to give a dark orange suspension. The suspension was filtered to remove inorganic salts, and the resulting solution was brought to dryness under a vacuum to give an oily residue, which was purified by column chromatography over silica gel eluting with dichloromethane. The obtained red, oily residue was disaggregated by stirring with cold pentane. The solid was filtered, washed with pentane (2 × 10 mL), and dried under a vacuum.

[RhI$_2${κ⁴*C*,*C*′,*N*,*N*′-(CH$_2$CMe$_2$ImCH$_2$PyCH$_2$NEt$_2$)}] (9). $[Rh(\mu\text{-Cl})(cod)]_2$ (129 mg, 0.262 mmol), [^{t}BuHImCH$_2$PyCH$_2$NEt$_2$]Br (200 mg, 0.524 mmol), KI (347.0 mg, 2.090 mmol) and KOAc (411.0 mg, 4.188 mmol). Yield: 76 mg, 22% (orange solid). Anal. Calcd for $C_{18}H_{27}I_2N_4Rh$: C, 32.95; H, 4.15; N, 8.54. Found: C, 32.95; H, 3.90; N, 8.48. HRMS (ESI+, MeOH, m/z): calcd for $C_{18}H_{27}I_2N_4Rh$: 655.9380; found, 529.0344 $[M - I]^+$, 401.1232 $[M - 2I - H]^+$. ^1H NMR (400 MHz, $CDCl_3$, 298 K): δ 7.69 (t, J_{H-H} = 7.8 Hz, 1H, H_p Py), 7.32 (d, J_{H-H} = 7.8 Hz, 2H, H_m Py, H_m Py), 7.04 (d, J_{H-H} = 2.1 Hz, 1H, =CH Im), 6.94 (d, J_{H-H} = 2.1 Hz, 1H, =CH Im), 5.64 (s, 2H, CH_2Im), 4.49 (s, 2H, CH_2NEt_2), 3.95 (d, 2H, J_{H-Rh} = 4.0 Hz, ImC(CH$_3$)$_2$CH_2−Rh), 3.75−3.63 (m, 2H, CH_2 Et), 3.17 (m, 2H, CH_2 Et), 1.58 (s, 6H, ImC(CH_3)$_2$CH$_2$−Rh), 1.13 (t, J_{H-H} = 7.1 Hz, 6H, CH_3 Et). $^{13}C\{^1H\}$ NMR (100.6 MHz, $CDCl_3$, 298 K): δ 166.0 (d, J_{C-Rh} = 34.3 Hz, C_{NCN}), 161.6, 152.7 (C_o Py), 137.7 (C_p Py), 123.1 (C_m Py), 121.4 (=CH Im), 121.3 (C_m Py), 118.1 (=CH Im), 66.6 (ImC(CH$_3$)$_2$CH$_2$−Rh), 63.9 (CH_2NEt_2), 55.7 (CH_2Im), 51.6 (CH_2 Et), 30.0 (ImC(CH$_3$)$_2$CH$_2$−Rh), 21.5 (d, J_{C-Rh} = 18.6 Hz, ImC(CH$_3$)$_2$CH$_2$−Rh), 10.1 (CH_3 Et).

[IrI$_2${κ⁴*C*,*C*′,*N*,*N*′-(CH$_2$CMe$_2$ImCH$_2$PyCH$_2$NHEt)}] (10). $[Ir(\mu\text{-Cl})(cod)]_2$ (175 mg, 0.261 mmol), [^{t}BuHImCH$_2$PyCH$_2$NEt$_2$]Br (200 mg, 0.524 mmol), KI (347.0 mg, 2.090 mmol) and KOAc (411.0 mg, 4.188 mmol). Yield: 38 mg, 10% (red solid). Anal. Calcd for $C_{16}H_{23}I_2N_4Ir$: C, 26.79; H, 3.23; N, 7.81. Found: C, 27.01; H, 3.55; N, 7.96. HRMS (ESI+, MeOH, m/z): calcd for $C_{16}H_{23}I_2N_4Ir$: 717.9642; found, 716.9711 $[M - H]^+$, 591.0584 $[M - I]^+$. ^1H NMR (300 MHz, $CDCl_3$, 298 K): δ 7.65 (t, J_{H-H} = 7.8 Hz, 1H, H_p Py), 7.35 (d, J_{H-H} = 7.8 Hz, 1H, H_m Py), 7.26 (d, J_{H-H} = 7.6 Hz, 1H, H_m Py), 6.95 (d, J_{H-H} = 2.2 Hz, 1H, =CH Im), 6.80 (d, J_{H-H} = 2.1 Hz, 1H, =CH Im), 6.03 (d, J_{H-H} = 16.4 Hz, 1H, CH_2Im), 5.60 (d, J_{H-H} = 16.4 Hz, 1H, CH_2Im), 4.65 (d, J_{H-H} = 10.3 Hz, 1H, CH_2NHEt), 4.58 (m, 2H, ImC(CH$_3$)$_2$CH_2−Ir), 4.48 (d, J_{H-H} = 10.2 Hz, 1H, CH_2NHEt), 4.31 (br, 1H, NH), 3.69−3.52 (m, 1H, CH_2 Et), 3.35−3.16 (m, 1H, CH_2 Et), 1.56 (s, 3H, ImC(CH_3)$_2$CH$_2$−Ir), 1.46 (s, 3H, ImC(CH_3)$_2$CH$_2$−Ir), 1.30 (t, J_{H-H} = 7.2 Hz, 3H, CH_3 Et). $^{13}C\{^1H\}$ NMR (75 MHz, $CDCl_3$, 298 K): δ 162.4, 151.8 (C_o Py), 145.9 (C_{NCN}), 136.4, (C_p Py), 123.5, 120.3 (C_m Py), 119.6, 117.2 (=CH Im), 67.1 (ImC(CH$_3$)$_2$CH$_2$−Ir), 60.9 (PyCH$_2$NHEt), 55.2 (CH_2Im), 49.9 (CH_2 Et), 31.9, 31.0 (ImC(CH$_3$)$_2$CH$_2$−Ir), 14.5 (CH_3 Et), 4.6 (ImC(CH$_3$)$_2$CH$_2$−Ir).

[RhI$_2${κ⁴*C*,*C*′,*N*,*N*′-(CH$_2$CMe$_2$ImCH$_2$PyCH$_2$NH^{t}Bu)}] (11). $[Rh(\mu\text{-Cl})(cod)]_2$ (129 mg, 0.262 mmol), [^{t}BuHImCH$_2$PyCH$_2$NH^{t}Bu]Br (200 mg, 0.524 mmol), KI (347.0 mg, 2.090 mmol) and KOAc

https://doi.org/10.1021/acs.organomet.3c00403
Organometallics 2023, 42, 3292−3306

(411.0 mg, 4.188 mmol). Yield: 83 mg, 24% (orange solid). Anal. Calcd for $C_{18}H_{27}I_2N_4Rh$: C, 32.95; H, 4.15; N, 8.54. Found: C, 33.07; H, 4.38; N, 8.25. HRMS (ESI+, MeOH, m/z): calcd for $C_{18}H_{27}I_2N_4Rh$: 655.9380; found, 529.0315 $[M - I]^+$. ^1H NMR (300 MHz, $CDCl_3$, 298 K): δ 7.70 (t, J_{H-H} = 7.8 Hz, 1H, H_p Py), 7.35 (d, J_{H-H} = 8.2 Hz, 1H, H_m Py), 7.31 (d, J_{H-H} = 7.8 Hz, 1H, H_m Py), 7.03 (d, J_{H-H} = 1.8 Hz, 1H, =CH Im), 6.92 (d, J_{H-H} = 1.7 Hz, 1H, =CH Im), 5.77 (d, J_{H-H} = 15.9 Hz, 1H, CH_2Im), 5.35 (d, J_{H-H} = 15.9 Hz, 1H, CH_2Im), 4.88−4.75 (m, 1H, CH_2NH^{t}Bu), 4.44−4.34 (m, 1H, CH_2NH^{t}Bu), 3.97 (s, 1H, NH), 3.93 (d, J_{H-H} = 3.1 Hz, 2H, ImC$(CH_3)_2CH_2$−Rh), 1.62 (s, 3H, ImC$(CH_3)_2CH_2$−Rh), 1.50 (s, 3H, ImC$(CH_3)_2CH_2$−Rh), 1.49 (s, 9H, ^{t}BuNH). $^{13}C\{^1H\}$ NMR (75 MHz, $CDCl_3$, 298 K): δ 169.2 (d, J_{C-Rh} = 35.8 Hz, C_{NCN}), 161.5, 151.9 (C_o Py), 137.7 (C_p Py), 123.3, 121.3 (C_m Py), 121.2, 117.8 (=CH Im), 66.8 (ImC$(CH_3)_2CH_2$−Rh), 56.9 (C ^{t}BuNH), 55.2 (CH_2Im), 53.7 (CH_2NH^{t}Bu), 31.0 (ImC$(CH_3)_2CH_2$−Rh), 29.7 (CH_3, ^{t}BuNH), 29.2 (ImC$(CH_3)_2CH_2$−Rh), 22.7 (d, J_{C-Rh} = 19.5 Hz, ImC$(CH_3)_2CH_2$−Rh).

[IrI$_2$\{κ^4*C,C′,N,N′*-(CH$_2$CMe$_2$ImCH$_2$PyCH$_2$NH^{t}Bu)\}] (12). $[Ir(\mu\text{-}Cl)(cod)]_2$ (175 mg, 0.262 mmol), [^{t}BuHImCH$_2$PyCH$_2$NH^{t}Bu]Br (200 mg, 0.524 mmol), KI (347.0 mg, 2.090 mmol) and KOAc (411.0 mg, 4.188 mmol). Yield: 51 mg, 13% (red solid). Anal. Calcd for $C_{18}H_{27}I_2N_4Ir$: C, 29.00; H, 3.65; N, 7.52. Found: C, 28.76; H, 3.73; N, 7.22. HRMS (ESI+, MeOH, m/z): calcd for $C_{18}H_{27}I_2N_4Ir$: 745.9955; found, 745.9939 $[M]^+$. ^1H NMR (300 MHz, $CDCl_3$, 298 K): δ 7.76 (t, J_{H-H} = 7.8 Hz, 1H, H_p Py), 7.42 (d, J_{H-H} = 7.8 Hz, 1H, H_m Py), 7.28 (d, J_{H-H} = 7.7 Hz, 1H, H_m Py), 6.95 (d, J_{H-H} = 2.1 Hz, 1H, =CH Im), 6.81 (d, J_{H-H} = 2.1 Hz, 1H, =CH Im), 6.12 (d, J_{H-H} = 16.0 Hz, 1H, CH_2Im), 5.42 (d, J_{H-H} = 16.4 Hz, 1H, CH_2Im), 4.86−4.78 (m, 1H, CH_2NH^{t}Bu), 4.66−4.52 (m, 3H, CH_2NH^{t}Bu, ImC$(CH_3)_2CH_2$−Ir), 4.40−4.30 (m, 1H, NH), 1.60 (s, 3H, ImC$(CH_3)_2CH_2$−Ir), 1.48 (s, 9H, ^{t}BuNH), 1.46 (s, 3H, ImC-$(CH_3)_2CH_2$−Ir). $^{13}C\{^1H\}$ NMR (75 MHz, $CDCl_3$, 298 K): δ 163.0 152.6 (C_o Py), 149.3 (C_{NCN}), 136.6 (C_p Py), 123.7, 121.4 (C_m Py), 119.9, 117.1 (=CH Im), 67.1 (ImC$(CH_3)_2CH_2$−Ir), 58.9 (C ^{t}BuNH), 55.6 (CH_2NH^{t}Bu), 55.1 (CH_2Im), 32.3, 30.7 (ImC-$(CH_3)_2CH_2$−Ir), 29.4 (CH_3, ^{t}BuNH), 5.6 ImC$(CH_3)_2CH_2$−Ir).

[IrH(CH$_3$CN)\{κ^4*C,C′,N,N′*-(CH$_2$CMe$_2$ImCH$_2$PyCH$_2$NEt$_2$)\}]PF$_6$ (13). A solution of [Ir(cod)(κ^3*C,N,N′*-^{t}BuImCH$_2$PyCH$_2$NEt$_2$)]PF_6 (**5**) (25 mg, 0.033 mmol) in CH_3CN (1 mL) was heated at 353 K for 24 h. The resulting yellow solution was brought to dryness in vacuo to give an oily residue that was disaggregated by stirring with cold Et_2O/hexane (1:1). The pale-yellow solid was filtered, washed with hexane (2 × 2 mL), and dried under vacuum. Yield: 17 mg, 78%. HRMS (ESI+, MeOH, m/z): calcd for $C_{20}H_{31}N_5Ir$: 534.2209; found, 493.1943 $[M - CH_3CN]^+$, 492.1867 $[M-CH_3CN-H]^+$. ^1H NMR (300 MHz, CD_3CN, 298 K): δ 7.87 (t, J_{H-H} = 7.8 Hz, 1H, H_p Py), 7.51 (d, J_{H-H} = 7.8 Hz, 1H, H_m Py), 7.39 (d, J_{H-H} = 7.8 Hz, 1H, H_m Py), 7.10 (d, J_{H-H} = 2.1 Hz, 1H, =CH Im), 6.96 (d, J_{H-H} = 2.1 Hz, 1H, =CH Im), 5.61 (ABq, δ_A = 5.49, δ_B = 5.73, J_{A-B} = 16.8 Hz, 2H, CH_2Im), 4.21 (ABq, δ_A = 4.31, δ_B = 4.12, J_{A-B} = 16.0 Hz, 2H, CH_2NEt_2), 3.27−3.02 (set of m, 2H, CH_2 Et), 2.59 (ABq, δ_A = 2.61, δ_B = 2.57, J_{A-B} = 10.4 Hz, 2H, ImC$(CH_3)_2CH_2$−Ir), 1.52 (s, 3H, ImC$(CH_3)_2CH_2$−Ir), 1.25 (s, 3H, ImC$(CH_3)_2CH_2$−Ir), 1.25 (t, J_{H-H} = 7.2 Hz, 3H, CH_3 Et), 1.08 (t, J_{H-H} = 7.2 Hz, 3H, CH_3 Et), −20.74 (s, 1H, Ir−H). $^{13}C\{^1H\}$ NMR (75 MHz, CD_3CN, 298 K): δ 185.07 (C_{NCN}), 137.8 (C_p Py), 124.9, 122.4 (C_m Py), 120.5, 117.1 (=CH Im), 68.4 (CH_2NEt_2), 55.3 (CH_2Im), 56.8, 52.2 (CH_2 Et), 30.6, 29.4 (ImC$(CH_3)_2CH_2$−Ir), 10.7 (ImC$(CH_3)_2CH_2$−Ir), 11.4, 9.7 (CH_3 Et).

Crystal Structure Determination. Single crystals were obtained by slow diffusion of pentane into a concentrated solution of the complexes in dichloromethane (**5**) or tetrahydrofuran (**9**−**12**). Single crystals of **6** were obtained by the slow diffusion of diethyl ether into a concentrated solution of the complex in chloroform. X-ray diffraction data were collected at 100(2) K on a Bruker APEX SMART diffractometer with graphite-monochromated Mo Kα radiation (λ = 0.71073 Å) using ω rotations. Intensities were integrated and corrected for absorption effects with the SAINT−PLUS[38] and SADABS[39] programs, both included in the APEX2 package. The structures were solved by the Patterson method with SHELXS-97[40] and refined by full matrix least-squares on F^2 with SHELXL-2014[41] under WinGX.[42] Pitch and yaw angles were calculated according to the literature.[43]

Crystal Data and Structure Refinement for 5. $C_{56}H_{90}F_{12}Ir_2N_8OP_2$, 1565.69 g·mol^{-1}, monoclinic, $C2/c$, a = 20.5251(10) Å, b = 18.0985(8) Å, c = 16.6726(8) Å, β = 100.5460(10)°, V = 6088.8(5) Å^3, Z = 4, D_{calc} = 1.708 g·cm^{-3}, μ = 4.502 mm^{-1}, F(000) = 3128, yellow prism, 0.210 × 0.130 × 0.090 mm^3, $\theta_{min}/\theta_{max}$ 1.836/28.616°, $-26 \le h \le 26$, $-23 \le k \le 23$, $-22 \le l \le 22$, reflections collected/independent 35,110/7352 [R(int) = 0.0359], T_{min}/T_{max} 0.5264/0.4090, data/restraints/parameters 7352/6/370, GooF(F^2) 1.049, R_1 = 0.0235 [$I > 2\sigma(I)$], wR_2 = 0.0496 (all data), largest diff. peak/hole 0.941/−0.522 e·Å^{-3}. CCDC deposit number 2266776.

Crystal Data and Structure Refinement for 6. $C_{19}H_{28}BrN_4ORh$, 511.27 g·mol^{-1}, monoclinic, $P2_1/n$, a = 11.7137(8) Å, b = 12.4294(8) Å, c = 14.5274(10) Å, β = 92.4310(10)°, V = 2113.2(2) Å^3, Z = 4, D_{calc} = 1.607 g·cm^{-3}, μ = 2.714 mm^{-1}, F(000) = 1032, yellow prism, 0.210 × 0.200 × 0.090 mm^3, $\theta_{min}/\theta_{max}$ 2.157/26.372°, $-14 \le h \le 14$, $-15 \le k \le 15$, $-18 \le l \le 18$, reflections collected/independent 44,159/4329 [R(int) = 0.0385], T_{min}/T_{max} 0.6381/0.5158, data/restraints/parameters 4329/0/240, GooF(F^2) = 1.043, R_1 = 0.0205 [$I > 2\sigma(I)$], wR_2 = 0.0509 (all data), largest diff. peak/hole 0.429/−0.474 e·Å^{-3}. CCDC deposit number 2266779.

Crystal Data and Structure Refinement for 9. $C_{22}H_{35}I_2N_4ORh$, 728.25 g·mol^{-1}, orthorhombic, $P2_12_12_1$, a = 11.3461(6) Å, b = 11.8058(6) Å, c = 19.5556(11) Å, V = 2619.5(2) Å^3, Z = 4, D_{calc} = 1.847 g·cm^{-3}, μ = 3.029 mm^{-1}, F(000) = 1416, red prism, 0.320 × 0.190 × 0.180 mm^3, $\theta_{min}/\theta_{max}$ 2.075/28.647°, $-15 \le h \le 14$, $-15 \le k \le 15$, $-25 \le l \le 26$, reflections collected/independent 44,609/6397 [R(int) = 0.0377], T_{min}/T_{max} 0.4922/0.4043, data/restraints/parameters 6397/0/230, GooF(F^2) = 1.062, R_1 = 0.0177 [$I > 2\sigma(I)$], wR_2 = 0.0398 (all data), absolute structure parameter −0.0258(8), largest diff. peak/hole 1.016/−0.417 e·Å^{-3}. CCDC deposit number 2266777.

Crystal Data and Structure Refinement for 10. $C_{16}H_{23}I_2IrN_4$, 717.38 g·mol^{-1}, Monoclinic, $P2_1$, a = 8.2072(6) Å, b = 13.6330(10) Å, c = 18.2105(13) Å, β = 97.8340(10)°, V = 2018.5(3) Å^3, Z = 4, D_{calc} = 2.361 g·cm^{-3}, μ = 9.678 mm^{-1}, F(000) = 1320, orange prism, 0.240 × 0.130 × 0.040 mm^3, $\theta_{min}/\theta_{max}$ 2.505/26.372°, $-10 \le h \le 10$, $-17 \le k \le 17$, $-22 \le l \le 22$, reflections collected/independent 21,697/8238 [R(int) = 0.0418], T_{min}/T_{max} 0.4043/0.2217, data/restraints/parameters 8238/1/421, GooF(F^2) = 0.847, R_1 = 0.0286 [$I > 2\sigma(I)$], wR_2 = 0.0621 (all data), absolute structure parameter 0.004(4), largest diff. peak/hole 1.665/−0.866 e·Å^{-3}. CCDC deposit number 2266774.

Crystal Data and Structure Refinement for 11. $C_{18}H_{27}I_2N_4Rh$, 656.14 g·mol^{-1}, monoclinic, $P2_1/c$, a = 12.8453(9) Å, b = 11.8681(8) Å, c = 17.1890(12) Å, β = 90.5160(10)°, V = 2620.3(3) Å^3, Z = 4, D_{calc} = 1.663 g·cm^{-3}, μ = 3.015 mm^{-1}, F(000) = 1256, orange prism, 0.330 × 0.150 × 0.125 mm^3, $\theta_{min}/\theta_{max}$ 1.585/28.648°, $-14 \le h \le 17$, $-15 \le k \le 15$, $-22 \le l \le 22$, reflections collected/independent 22,476/6183 [R(int) = 0.0315], T_{min}/T_{max} 0.5635/0.4220, data/restraints/parameters 6183/0/231, GooF(F^2) = 1.036, R_1 = 0.0251 [$I > 2\sigma(I)$], wR_2 = 0.0622 (all data), largest diff. peak/hole 0.634/−0.628 e·Å^{-3}. CCDC deposit number 2266778.

Crystal Data and Structure Refinement for 12. $C_{22}H_{35}I_2IrN_4O$, 817.54 g·mol^{-1}, monoclinic, $P2_1/c$, a = 12.8402(7) Å, b = 11.8331(7) Å, c = 17.2477(10) Å, β = 90.7630(10)°, V = 2620.4(3) Å^3, Z = 4, D_{calc} = 2.072 g·cm^{-3}, μ = 7.472 mm^{-1}, F(000) = 1544, orange prism, 0.280 × 0.090 × 0.075 mm^3, $\theta_{min}/\theta_{max}$ 1.586/27.878°, $-16 \le h \le 16$, $-15 \le k \le 15$, $-22 \le l \le 22$, reflections collected/independent 29,666/6166 [R(int) = 0.0306], T_{min}/T_{max} 0.3842/0.2287, data/restraints/parameters 6166/20/232, GooF(F^2) = 1.108, R_1 = 0.0213 [$I > 2\sigma(I)$], wR_2 = 0.0423 (all data), largest diff. peak/hole 1.119/−0.867 e·Å^{-3}. CCDC deposit number 2266775.

Computational Details. All computations were performed using the Gaussian 09 package.[44] The structures of the minima were fully

https://doi.org/10.1021/acs.organomet.3c00403
Organometallics 2023, 42, 3292−3306

optimized without geometrical constraints and confirmed by frequency calculations, and solvent effects (acetonitrile) were included. The calculations were carried out using the B3LYP functional with Grimme's D3 dispersion correction.[45,46] The basis set used for rhodium, iridium, and iodine was LANL2DZ and its associated ECP, supplemented with an f[47] function for rhodium and iridium and a d function[48] for iodine. For the rest of the atoms, the basis set 6-31G** was used.

■ ASSOCIATED CONTENT

Supporting Information

The Supporting Information is available free of charge at https://pubs.acs.org/doi/10.1021/acs.organomet.3c00403.

^{1}H and ^{13}C NMR spectra for the organometallic compounds, FTIR spectra, and DFT energy data (PDF)

Optimized coordinates for reaction intermediates (XYZ)

Accession Codes

CCDC 2266774−2266779 contain the supplementary crystallographic data for this paper. These data can be obtained free of charge via www.ccdc.cam.ac.uk/data_request/cif, or by emailing data_request@ccdc.cam.ac.uk, or by contacting The Cambridge Crystallographic Data Centre, 12 Union Road, Cambridge CB2 1EZ, UK; fax: +44 1223 336033.

■ AUTHOR INFORMATION

Corresponding Authors

M. Victoria Jiménez − *Departamento de Química Inorgánica, Instituto de Síntesis Química y Catálisis Homogénea-ISQCH, Universidad de Zaragoza-C.S.I.C., 50009 Zaragoza, Spain;* orcid.org/0000-0002-0545-9107; Email: vjimenez@unizar.es

Jesús J. Pérez-Torrente − *Departamento de Química Inorgánica, Instituto de Síntesis Química y Catálisis Homogénea-ISQCH, Universidad de Zaragoza-C.S.I.C., 50009 Zaragoza, Spain;* orcid.org/0000-0002-3327-0918; Email: perez@unizar.es

Authors

Miguel González-Lainez − *Departamento de Química Inorgánica, Instituto de Síntesis Química y Catálisis Homogénea-ISQCH, Universidad de Zaragoza-C.S.I.C., 50009 Zaragoza, Spain*

Vincenzo Passarelli − *Departamento de Química Inorgánica, Instituto de Síntesis Química y Catálisis Homogénea-ISQCH, Universidad de Zaragoza-C.S.I.C., 50009 Zaragoza, Spain;* orcid.org/0000-0002-1735-6439

F. Javier Modrego − *Departamento de Química Inorgánica, Instituto de Síntesis Química y Catálisis Homogénea-ISQCH, Universidad de Zaragoza-C.S.I.C., 50009 Zaragoza, Spain;* orcid.org/0000-0002-9633-3285

Complete contact information is available at: https://pubs.acs.org/10.1021/acs.organomet.3c00403

Author Contributions

The manuscript was written through the contributions of all authors. All authors have given approval to the final version of the manuscript.

Notes

The authors declare no competing financial interest.

■ ACKNOWLEDGMENTS

The authors express their appreciation for the financial support from the Spanish Ministerio de Ciencia e Innovación, MCIN/AEI/10.13039/501100011033, under the project PID2019-103965GB-I00, and the "Departamento de Ciencia, Universidad y Sociedad del Conocimiento del Gobierno de Aragón" (group E42_23R). M.G.-L. thanks the Spanish Ministerio de Economía y Competitividad (MINECO) for a predoctoral fellowship (BES-2014-069624).

■ REFERENCES

(1) (a) *Organometallic Pincer Chemistry*; van Koten, G., Milstein, D., Eds.; Springer-Verlag: Heidelberg, 2013. (b) *Pincer Compounds, Chemistry and Applications*; Morales-Morales, D., Ed.; Elsevier Science: Amsterdam, 2018. (c) *Pincer-Metal Complexes: Applications in Catalytic Dehydrogenation Chemistry*; Kumar, A., Ed.; Elsevier: Amsterdam, 2022.

(2) (a) *The Chemistry of Pincer Compounds*; Morales-Morales, D., Jensen, C. M., Eds.; Elsevier Science: Amsterdam, 2007. (b) *The Privileged Pincer-Metal Platform: Coordination Chemistry & Applications*; van Koten, G., Gossage, R., Eds.; Topics in Organometallic Chemistry: Heidelberg, 2016; Vol. *54*.

(3) (a) Herrmann, W. N-Heterocyclic Carbenes: A New Concept in Organometallic Catalysis. *Angew. Chem., Int. Ed.* **2002**, *41*, 1290−1309. (b) Díez-González, S.; Marion, N.; Nolan, S. P. N-Heterocyclic Carbenes in Late Transition Metal Catalysis. *Chem. Rev.* **2009**, *109*, 3612−3676. (c) Peris, E. Smart N-Heterocyclic Carbene Ligands in Catalysis. *Chem. Rev.* **2018**, *118*, 9988−10031. (d) Lee, J.; Hahm, H.; Kwak, J.; Kim, M. New Aspects of Recently Developed Rhodium(N-Heterocyclic Carbene)-Catalyzed Organic Transformations. *Adv. Synth. Catal.* **2019**, *361*, 1479−1499.

(4) (a) Doris Kunz, D.; Jürgens, E. Strongly Electron Donating Tridentate N-Heterocyclic Biscarbene Ligands for Rhodium and Iridium Catalysts. In *Molecular Catalysts: Structure and Functional Design*; Gade, L. H., Hofmann, P., Eds.; Wiley-VCH, 2014; pp 183−186. (b) Farrell, K.; Albrecht, M. Late Transition Metal Complexes with Pincer Ligands that Comprise *N*-Heterocyclic Carbene Donor Sites. *Top. Organomet. Chem.* **2015**, *54*, 45−91.

(5) (a) Milstein, D. Discovery of Environmentally Benign Catalytic Reactions of Alcohols Catalyzed by Pyridine-Based Pincer Ru Complexes Based on Metal-Ligand Cooperation. *Top. Catal.* **2010**, *53*, 915−923. (b) Gunanathan, C.; Milstein, D. Metal-Ligand Cooperation by Aromatization-Dearomatization: A New Paradigm in Bond Activation and "Green" Catalysis. *Acc. Chem. Res.* **2011**, *44*, 588−602. (c) Gunanathan, C.; Milstein, D. Bond Activation and Catalysis by Ruthenium Pincer Complexes. *Chem. Rev.* **2014**, *114*, 12024−12087. (d) Milstein, D. Metal-Ligand Cooperation by Aromatization-Dearomatization as a Tool in Single Bond Activation. *Philos. Trans. R. Soc., A* **2015**, *373*, 20140189.

(6) (a) Filonenko, G. A.; Cosimi, E.; Lefort, L.; Conley, M. P.; Copéret, C.; Lutz, M.; Hensen, E. J. M.; Pidko, E. A. Lutidine-Derived Ru- CNC Hydrogenation Pincer Catalysts with Versatile Coordination Properties. *ACS Catal.* **2014**, *4*, 2667−2671. (b) Hermosilla, P.; García-Orduña, P.; Lahoz, F. J.; Polo, V.; Casado, M. A. Rh Complexes with Pincer Carbene CNC Lutidine-Based Ligands: Reactivity Studies toward H_2 Addition. *Organometallics* **2021**, *40*, 3720−3732. (c) Hermosilla, P.; García-Orduña, P.; Sanz Miguel, P. J.; Polo, V.; Casado, M. A. Nucleophilic Reactivity at a = CH Arm of a Lutidine-Based CNC/Rh System: Unusual Alkyne and CO_2 Activation. *Inorg. Chem.* **2022**, *61*, 7120−7129.

(7) (a) Inamoto, K.; Kuroda, J.-I.; Kwon, E.; Hiroya, K.; Doi, T. Pincer-type bis(carbene)-derived complexes of nickel(II): Synthesis, structure, and catalytic activity. *J. Organomet. Chem.* **2009**, *694*, 389−396. (b) Hernández-Juárez, M.; López-Serrano, J.; Lara, P.; Morales-Cerón, J. P.; Vaquero, M.; Álvarez, E.; Salazar, V.; Suárez, A. Ruthenium(II) Complexes Containing Lutidine-Derived Pincer CNC Ligands: Synthesis, Structure, and Catalytic Hydrogenation of C-N

bonds. *Chem.—Eur. J.* **2015**, *21*, 7540−7555. (c) Storey, C. M.; Kalpokas, A.; Gyton, M. R.; Krämer, T.; Chaplin, A. B. A Shape Changing Tandem Rh(CNC) Catalyst: Preparation of Bicyclo[4.2.0]-Octa-1,5,7-Trienes from Terminal Aryl Alkynes. *Chem. Sci.* **2020**, *11*, 2051−2057. (d) Hermosilla, P.; Urriolabeitia, A.; Iglesias, M.; Polo, V.; Casado, M. A. Efficient solventless dehydrogenation of formic acid by a CNC-based rhodium catalyst. *Inorg. Chem. Front.* **2022**, *9*, 4538−4547.

(8) Dey, S.; Rawat, M.; Hollis, T. K. Carbene-Based Pincer Ligands. In *Comprehensive Coordination Chemistry III*; Constable, E. C., Parkin, G., QueJr, L., Eds.; Elsevier, 2021; pp 607−649.

(9) Boronat, M.; Corma, A.; González-Arellano, C.; Iglesias, M.; Sánchez, F. Synthesis of Electron-Rich CNN-Pincer Complexes with N-Heterocyclic Carbene and (*S*)-Proline Moieties and Application to Asymmetric Hydrogenation. *Organometallics* **2010**, *29*, 134−141.

(10) (a) Del Pozo, C.; Corma, A.; Iglesias, M.; Sánchez, F. Immobilization of (NHC)NN-Pincer Complexes on Mesoporous MCM-41 Support. *Organometallics* **2010**, *29*, 4491−4498. (b) Del Pozo, C.; Corma, A.; Iglesias, M.; Sánchez, F. Recyclable mesoporous silica-supported chiral ruthenium-(NHC)NN-pincer catalysts for asymmetric reactions. *Green Chem.* **2011**, *13*, 2471−2481. (c) Del Pozo, C.; Iglesias, M.; Sánchez, F. Pincer-type Pyridine-Based N-Heterocyclic Carbene Amine Ru(II) Complexes as Efficient Catalysts for Hydrogen Transfer Reactions. *Organometallics* **2011**, *30*, 2180−2188.

(11) Sun, Y.; Koehler, C.; Tan, R.; Annibale, V. T.; Song, D. Ester hydrogenation catalyzed by Ru-CNN pincer complexes. *Chem. Commun.* **2011**, *47*, 8349−8351.

(12) González-Lainez, M.; Gallegos, M.; Munarriz, J.; Azpiroz, R.; Passarelli, V.; Jiménez, M. V.; Pérez-Torrente, J. J. Copper-Catalyzed Azide-Alkyne Cycloaddition (CuAAC) by Functionalized NHC-Based Polynuclear Catalysts: Scope and Mechanistic Insights. *Organometallics* **2022**, *41*, 2154−2169.

(13) (a) Sánchez, P.; Hernández-Juárez, M.; Rendón, N.; López-Serrano, J.; Santos, L. L.; Álvarez, E.; Paneque, M.; Suárez, A. Hydrogenation/dehydrogenation of N-heterocycles catalyzed by ruthenium complexes based on multimodal proton-responsive CNN(H) pincer ligands. *Dalton Trans.* **2020**, *49*, 9583−9587. (b) Ortega-Lepe, I.; Rossin, A.; Sánchez, P.; Santos, L. L.; Rendón, N.; Alvarez, E.; López-Serrano, J.; Suárez, A. Ammonia-Borane Dehydrogenation Catalyzed by Dual-Mode Proton-Responsive Ir-CNNH Complexes. *Inorg. Chem.* **2021**, *60*, 18490−18502.

(14) Zeng, F.; Yu, Z. Pyridyl-Supported Pyrazolyl-N-Heterocyclic Carbene Ligands and the Catalytic Activity of Their Palladium Complexes in Suzuki-Miyaura Reactions. *J. Org. Chem.* **2006**, *71*, 5274−5281.

(15) Sánchez, P.; Hernández-Juárez, M.; Álvarez, E.; Paneque, M.; Rendón, N.; Suárez, A. Synthesis, Structure and Reactivity of Pd and Ir Complexes Based on New Lutidine-Derived NHC/Phosphine Mixed Pincer Ligands. *Dalton Trans.* **2016**, *45*, 16997−17009.

(16) Hernández-Juárez, M.; López-Serrano, J.; González-Herrero, P.; Rendón, N.; Álvarez, E.; Paneque, M.; Suárez, A. Hydrogenation of an Iridium-Coordinated Imidazole-2-ylidene Ligand Fragment. *Chem. Commun.* **2018**, *54*, 3843−3846.

(17) (a) Sánchez, P.; Hernández-Juárez, M.; Rendón, N.; López-Serrano, J.; Álvarez, E.; Paneque, M.; Suárez, A. Hydroboration of Carbon Dioxide with Catechol and Pinacol Borane Using an Ir-CNP* Pincer Complex. Water Influence on the Catalytic Activity. *Dalton Trans.* **2018**, *47*, 16766−16776. (b) Sánchez, P.; Hernández-Juárez, M.; Rendón, N.; López-Serrano, J.; Álvarez, E.; Paneque, M.; Suárez, A. Selective, Base-Free Hydrogenation of Aldehydes Catalyzed by Ir Complexes Based on Proton-Responsive Lutidine-Derived CNP Ligands. *Organometallics* **2021**, *40*, 1314−1327.

(18) (a) González-Lainez, M.; Jiménez, M. V.; Passarelli, V.; Pérez-Torrente, J. J. Effective N-methylation of nitroarenes with methanol catalyzed by a functionalized NHC-based iridium catalyst: a green approach to N-methyl amines. *Catal. Sci. Technol.* **2020**, *10*, 3458−3467. (b) González-Lainez, M.; Jiménez, M. V.; Azpiroz, R.; Passarelli, V.; Modrego, F. J.; Pérez-Torrente, J. J. N-Methylation of Amines with Methanol Catalyzed by Iridium(I) Complexes Bearing an N,O-Functionalized NHC Ligand. *Organometallics* **2022**, *41*, 1364−1380. (c) González-Lainez, M.; Jiménez, M. V.; Passarelli, V.; Pérez-Torrente, J. J. β-(*Z*)-Selective alkyne hydrosilylation by a N,O-functionalized NHC-based rhodium(I) catalyst. *Dalton Trans.* **2023**, *52*, 11503−11517.

(19) (a) Frey, G. D.; Rentzsch, C. F.; von Preysing, D.; Scherg, T.; Mühlhofer, M.; Herdtweck, E.; Herrmann, W. A. Rhodium and iridium complexes of N-heterocyclic carbenes: Structural investigations and their catalytic properties in the borylation reaction. *J. Organomet. Chem.* **2006**, *691*, 5725−5738. (b) Straubinger, C. S.; Jokić, N. B.; Högerl, M. P.; Herdtweck, E.; Herrmann, W. A.; Kühn, F. E. Bridge functionalized bis-N-heterocyclic carbene rhodium(I) complexes and their application in catalytic hydrosilylation. *J. Organomet. Chem.* **2011**, *696*, 687−692.

(20) (a) Jiménez, M. V.; Fernández-Tornos, J.; Perez-Torrente, J. J.; Modrego, F. J.; Winterle, S.; Cunchillos, C.; Lahoz, F.; Oro, L. A. Iridium(I) Complexes with Hemilabile N-Heterocyclic Carbenes: Efficient and Versatile Transfer Hydrogenation Catalysts. *Organometallics* **2011**, *30*, 5493−5508. (b) Angoy, M.; Jiménez, M. V.; Lahoz, F. J.; Vispe, E.; Pérez-Torrente, J. J. Polymerization of phenylacetylene catalyzed by rhodium(I) complexes with *N*-functionalized N-heterocyclic carbene ligands. *Polymer Chem.* **2022**, *13*, 1411−1421.

(21) Albrecht, M.; Miecznikowski, J. R.; Samuel, A.; Faller, J. W.; Crabtree, R. H. Chelated Iridium(III) Bis-carbene Complexes as Air-Stable Catalysts for Transfer Hydrogenation. *Organometallics* **2002**, *21*, 3596−3604.

(22) (a) Albrecht, M.; Crabtree, R. H.; Mata, J.; Peris, E. Chelating bis-carbene rhodium(iii) complexes in transfer hydrogenation of ketones and iminesElectronic supplementary information (ESI) available: spectroscopic data for the rhodium(iii) complexes. *Chem. Commun.* **2002**, 32−33. (b) Krüger, A.; Häller, L. J. L.; Müller-Bunz, H.; Serada, O.; Neels, A.; Macgregor, S. A.; Albrecht, M. Smooth C(alkyl)-H bond activation in rhodium complexes comprising abnormal carbene ligands. *Dalton Trans.* **2011**, *40*, 9911−9920. (c) Iglesias, M.; Pérez-Nicolás, M.; Miguel, P. J. S.; Polo, V.; Fernández-Alvarez, F. J.; Pérez-Torrente, J. J.; Oro, L. A. A synthon for a 14-electron Ir(III) species: catalyst for highly selective β-(Z) hydrosilylation of terminal alkynes. *Chem. Commun.* **2012**, *48*, 9480−9482. (d) Iglesias, M.; Sanz Miguel, P. J.; Polo, V.; Fernández-Alvarez, F. J.; Pérez-Torrente, J. J.; Oro, L. A. An Alternative Mechanistic Paradigm for the β-Z Hydrosilylation of Terminal Alkynes: The Role of Acetone as a Silane Shuttle. *Chem.—Eur. J.* **2013**, *19*, 17559−17566.

(23) (a) Dorta, R.; Stevens, E. D.; Nolan, S. P. Double C-H Activation in a Rh-NHC Complex Leading to the Isolation of a 14-Electron Rh(III) Complex. *J. Am. Chem. Soc.* **2004**, *126*, 5054−5055. (b) Scott, N. M.; Dorta, R.; Stevens, E. D.; Correa, A.; Cavallo, L.; Nolan, S. P. Interaction of a Bulky N-Heterocyclic Carbene Ligand with Rh(I) and Ir(I). Double C-H Activation and Isolation of Bare 14-Electron Rh(III) and Ir(III) Complexes. *J. Am. Chem. Soc.* **2005**, *127*, 3516−3526. (c) Corberán, R.; Sanaú, M.; Peris, E. Aliphatic and Aromatic Intramolecular C-H Activation on *Cp**Ir(NHC) Complexes. *Organometallics* **2006**, *25*, 4002−4008. (d) Wheatley, J. E.; Ohlin, C. A.; Chaplin, A. B. Solvent promoted reversible cyclometalation in a tethered NHC iridium complex. *Chem. Commun.* **2014**, *50*, 685−687. (e) Holmes, J.; Pask, C. M.; Willans, C. E. Chelating N-heterocyclic carbene-carboranes offer flexible ligand coordination to Ir^{III}, Rh^{III} and Ru^{II}: effect of ligand cyclometallation in catalytic transfer hydrogenation. *Dalton Trans.* **2016**, *45*, 15818−15827.

(24) (a) Morilla, M. E.; Morfes, G.; Nicasio, M. C.; Belderrain, T. R.; Díaz-Requejo, M. M.; Graiff, C.; Tiripicchio, A.; Sánchez-Delgado, R.; Pérez, P. J. Intramolecular dealkylation of chelating diamines with Ru(II) complexes. *Chem. Commun.* **2002**, 1848−1849. (b) Morilla, M. E.; Rodríguez, P.; Belderrain, T. R.; Graiff, C.; Tiripicchio, A.; Nicasio, M. C.; Pérez, P. J. Synthesis, Characterization, and Reactivity

https://doi.org/10.1021/acs.organomet.3c00403
Organometallics 2023, 42, 3292−3306

of Ruthenium Diene/Diamine Complexes Including Catalytic Hydrogenation of Ketones. *Inorg. Chem.* **2007**, *46*, 9405−9414.
(25) (a) Lapointe, D.; Fagnou, K. Overview of the Mechanistic Work on the Concerted Metallation-Deprotonation Pathway. *Chem. Lett.* **2010**, *39*, 1118−1126. (b) Jiang, J.; Ramozzi, R.; Morokuma, K. Rh^{III}-Catalyzed C(sp^3)-H Bond Activation by an External Base Metalation/Deprotonation Mechanism: A Theoretical Study. *Chem.—Eur. J.* **2015**, *21*, 11158−11164. (c) Shan, C.; Zhu, L.; Qu, L.-B.; Bai, R.; Lan, Y. Mechanistic view of Ru-catalyzed C-H bond activation and functionalization: computational advances. *Chem. Soc. Rev.* **2018**, *47*, 7552−7576. (d) McMullin, C. L.; Rajabi, N. A.; Hammerton, J. S. A computational study on the identity of the active catalyst structure for Ru(II) carboxylate assisted C-H activation in acetonitrile. *Org. Biomol. Chem.* **2019**, *17*, 6678−6686.
(26) (a) For a review of proton transfer reactions of metal hydrides, see:Kristjánsdóttir, S. S.; Norton, J. R. In *Transition Metal Hydrides*; Dedieu, A., Ed.; VCH: New York, 1992; Chpt. 9, pp 309−359. (b) Morris, R. H. Estimating the Acidity of Transition Metal Hydride and Dihydrogen Complexes by Adding Ligand Acidity Constants. *J. Am. Chem. Soc.* **2014**, *136*, 1948−1959.
(27) Goldberg, J. M.; Berman, J. L.; Kaminsky, W.; Goldberg, K. I.; Heinekey, D. M. Oxidative addition of iodine to (tBu)4(POCOP)-Ir(CO) complexes(*t*Bu)4(POCOP)Ir(CO) complexes. *J. Organomet. Chem.* **2017**, *845*, 171−176.
(28) Shaffer, D. W.; Ryken, S. A.; Zarkesh, R. A.; Heyduk, A. F. Ligand Effects on the Oxidative Addition of Halogens to (dpp-nacnac^R)Rh(phdi). *Inorg. Chem.* **2012**, *51*, 12122−12131.
(29) Fukuzumi, S.; Nishizawa, N.; Tanaka, T. Electron Transfer Activation in the Oxidative Addition of Iodine to Rhodium(I) Complexes. *Bull. Chem. Soc. Jpn.* **1982**, *55*, 2886−2891.
(30) Anslyn, E. V.; Dougherty, D. A. *Modern Physical Organic Chemistry*; University Science Books: Mill Valley, CA, 2006.
(31) Poyatos, M.; Sanau, M.; Peris, E. New Rh(I) and Rh(III) Bisimidazol-2-ylidene Complexes: Synthesis, Reactivity, and Molecular Structures. *Inorg. Chem.* **2003**, *42*, 2572−2576.
(32) (a) Poyatos, M.; Mas-Marzá, E.; Mata, J.; Sanau, M.; Peris, E. Synthesis, Reactivity, Crystal Structures and Catalytic Activity of New Chelating Bisimidazolium-Carbene Complexes of Rh. *Eur. J. Inorg. Chem.* **2003**, *2003*, 1215−1221. (b) Yang, L.; Krüger, A.; Neels, A.; Albrecht, M. Rhodium(III) Complexes Containing C4-Bound N-Heterocyclic Carbenes: Synthesis, Coordination Chemistry, and Catalytic Activity in Transfer Hydrogenation. *Organometallics* **2008**, *27*, 3161−3171.
(33) Albrecht, M.; Miecznikowski, J. R.; Samuel, A.; Faller, J. W.; Crabtree, R. H. Chelated Iridium(III) Bis-carbene Complexes as Air-Stable Catalysts for Transfer Hydrogenation. *Organometallics* **2002**, *21*, 3596−3604.
(34) Willems, S. T. H.; Russcher, J. C.; Budzelaar, P. H. M.; Bruin, B. d.; Gelder, R. d.; Smits, J. M. M.; W Gal, A. Spontaneous disproportionation of rhodium(i) bisoxazolinates to rhodium(ii)-Electronic supplementary information (ESI) available: synthetic procedures (including 1H NMR, 13C NMR and elemental analysis data), EPR spectrum and cyclic voltammogram. *Chem. Commun.* **2002**, 148−149.
(35) Giordano, G.; Crabtree, R. H.; Heintz, R. M.; Forster, D.; Morris, D. E. Di-μ-Chloro-Bis(η^4-1,5-Cyclooctadiene) Dirhodium(I), *Inorganic Syntheses*; John Wiley & Sons, Inc., 1979; Vol. *19*, pp 218−220.
(36) Herde, J. L.; Lambert, J. C.; Senoff, C. V.; Cushing, M. A. Cyclooctene and 1,5-Cyclooctadiene Complexes of Iridium(I) *Inorganic Syntheses*; John Wiley & Sons, Inc., 1974; Vol. *15*, pp 18−20.
(37) Usón, R.; Oro, L. A.; Cabeza, J. A.; Bryndza, H. E.; Stepro, M. P. Dinuclear Methoxy, Cyclooctadiene, and Barrelene Complexes of Rhodium(I) and Iridium(I). *Inorganic Syntheses*; John Wiley & Sons, Inc., 1985; Vol. *23*, pp 126−130.
(38) *SAINT+: Area-Detector Integration Software*, version 6.01; Bruker AXS: Madison, WI, 2001.
(39) Sheldrick, G. M. *SADABS Program*; University of Göttingen: Göttingen, Germany, 1999;.
(40) Sheldrick, G. M. *SHELXS 97, Program for the Solution of Crystal Structure*; University of Göttingen: Göttingen, Germany, 1997;.
(41) Sheldrick, G. M. Crystal structure refinement with SHELXL. *Acta Crystallogr., Sect. C: Struct. Chem.* **2015**, *71*, 3−8.
(42) Farrugia, L. J. WinGX and ORTEP for Windows: An Update. *J. Appl. Crystallogr.* **2012**, *45*, 849−854.
(43) Azpíroz, R.; Rubio-Pérez, L.; Di Giuseppe, A.; Passarelli, V.; Lahoz, F. J.; Castarlenas, R.; Pérez-Torrente, J. J.; Oro, L. A. Rhodium(I)-N-Heterocyclic Carbene Catalyst for Selective Coupling of *N*-Vinylpyrazoles with Alkynes via C-H Activation. *ACS Catal.* **2014**, *4*, 4244−4253.
(44) Frisch, M. J.; Trucks, G. W.; Schlegel, H. B.; Scuseria, G. E.; Robb, M. A.; Cheeseman, J. R.; Scalmani, G.; Barone, V.; Mennucci, B.; Petersson, G. A.; Nakatsuji, H.; Caricato, M.; Li, X.; Hratchian, H. P.; Izmaylov, A. F.; Bloino, J.; Zheng, G.; Sonnenberg, J. L.; Hada, M.; Ehara, M.; Toyota, K.; Fukuda, R.; Hasegawa, J.; Ishida, M.; Nakajima, T.; Honda, Y.; Kitao, O.; Nakai, H.; Vreven, T.; Montgomery, J. A.; Peralta, J. E.; Ogliaro, F.; Bearpark, M.; Heyd, J. J.; Brothers, E.; Kudin, K. N.; Staroverov, V. N.; Kobayashi, R.; Normand, J.; Raghavachari, K.; Rendell, A.; Burant, J. C.; Iyengar, S. S.; Tomasi, J.; Cossi, M.; Rega, N.; Millam, J. M.; Klene, M.; Knox, J. E.; Cross, J. B.; Bakken, V.; Adamo, C.; Jaramillo, J.; Gomperts, R.; Stratmann, R. E.; Yazyev, O.; Austin, A. J.; Cammi, R.; Pomelli, C.; Ochterski, J. W.; Martin, R. L.; Morokuma, K.; Zakrzewski, V. G.; Voth, G. A.; Salvador, P.; Dannenberg, J. J.; Dapprich, S.; Daniels, A. D.; Farkas; Foresman, J. B.; Ortiz, J. V.; Cioslowski, J.; Fox, D. J. *Gaussian 09*. Revision D.01; Gaussian, Inc.: Wallingford CT, 2009;.
(45) Grimme, S.; Antony, J.; Ehrlich, S.; Krieg, H. A consistent and accurate ab initio parametrization of density functional dispersion correction (DFT-D) for the 94 elements H-Pu. *J. Chem. Phys.* **2010**, *132*, 154104.
(46) Mateyise, N. G. S.; Conradie, J.; Conradie, M. M. Density functional theory calculated data of the iodomethane oxidative addition to oligothiophene-containing rhodium complexes - importance of dispersion correction. *Data in Brief* **2021**, *35*, 106929.
(47) Ehlers, A. W.; Böhme, M.; Dapprich, S.; Gobbi, A.; Höllwarth, A.; Jonas, V.; Köhler, K.; Stegmann, R.; Veldkamp, A.; Frenking, G. A set of f-polarization functions for pseudo-potential basis sets of the transition metals Sc-Cu, Y-Ag and La-Au. *Chem. Phys. Lett.* **1993**, *208*, 111−114.
(48) Check, C. E.; Faust, T. O.; Bailey, J. M.; Wright, B. J.; Gilbert, T. M.; Sunderlin, L. S. Addition of Polarization and Diffuse Functions to the LANL2DZ Basis Set for P-Block Elements. *J. Phys. Chem. A* **2001**, *105*, 8111−8116.

https://doi.org/10.1021/acs.organomet.3c00403
Organometallics 2023, 42, 3292−3306